

Coding with Action Potentials – Theory and Principles of Temporal Coding

Venue Ev. Begegnungsstätte Hirschluch (Storkow), Brandenburg
<http://web4.t-webby.de/hirschluch/>

Date Feb. 14/15, 2009 (arrival: Feb. 13, afternoon)

List of Participants

1	Brill	Martin	PhD	Wuerzburg, Biozentrum
2	Christian	Jan-Ole	MSc Bioinformatics	Berlin, FU
3	Clemens	Jan	PhD	Berlin, HU, BCCN
4	Daehne	Sven	MSc Comp. Neurosci.	Berlin, BCCN
5	Dold	Hannah	PhD	Berlin, TU, BCCN
6	Goergen	Kai	MSc Comp. Neurosci.	Berlin, BCCN
7	Felsenberg	Johannes	PhD	Berlin, FU
8	Franke	Felix	PhD	Berlin, TU, BCCN
9	Haeusler	Chris	MSc Comp. Neurosci.	Berlin, BCCN
11	Schönfelder	Vinzenz	PhD	Berlin, BCCN

Organization

Prof. Dr. Martin Nawrot
Neuroinformatics / Theoretical Neuroscience
Institute of Biology
Freie Universität Berlin

Dr. Michael Schmuker
Neurobiology
Institute of Biology
Freie Universität Berlin



Sponsoring

We acknowledge generous funding of this course by the
Bernstein Center for Computational Neuroscience Berlin

List of Topics

I Biophysical basis of temporal coding: Reliable timing of spikes and synaptic events

[1 **Jan Clemens** ✓]

Mainen, Z. F. & Sejnowski, T. J. (1995) *Reliability of spike timing in neocortical neurons*. *Science* **268**(5216), 1503--1506. [[patch clamp recording + noise current injection](#)]

[2 **Martin Nawrot** (replaces Lloyd Elliot)]

Nawrot MP, Schnepel P, Aertsen A, Boucsein C (2008) *Precisely timed signal transmission in neocortical networks with reliable intermediate-range projections*. (submitted) [[photostimulation](#)]

+ *additional paper that explains method in detail*

Boucsein C, Nawrot MP, Rotter S, Aertsen A, Heck D (2005) *Controlling synaptic input patterns in vitro by dynamic photo stimulation*. *J NeuroPhysiol* **94**: 2948-2958.

II Learning spike patterns: Spike Timing Dependent Plasticity & Tempotron

[3 **Martin Nawrot** (replaces Jakob Gutzmann) ✓] $\Rightarrow a (+ b)$

Bi GQ, Poo MM. (1998) *Synaptic modifications in cultured hippocampal neurons: dependence on spike timing, synaptic strength, and postsynaptic cell type*. *J Neurosci*. **18**(24):10464-72 (a) [[paired patch recording](#)]

Bi G, Poo M. (1999) *Distributed synaptic modification in neural networks induced by patterned stimulation*. *Nature*. **401**(6755):792-6. (b)

+ *additional review on this topic*

Bi, G. & Poo, M. (2001) *Synaptic modification by correlated activity: Hebb's postulate revisited*. *Annu Rev Neurosci* **24**, 139--166. (review)

[4 **Felix Franke** ✓]

Gütig, R. & Sompolinsky, H. (2006) *The tempotron: a neuron that learns spike timing-based decisions*. *Nat Neurosci* **9**(3), 420--428. (*model study*) [[leaky integrate and fire model neuron + Poisson process](#)]

+ *suggested article on background of integrate and fire neuron, e.g. Burkitt AN (2006) A review of the integrate-and-fire neuron model: I. Homogeneous synaptic input. Biol Cybern. 95:1-19*

[5 **Jan-Ole Christian** ✓] [Tutor: **Michael Schmuker**] *a or b – decide with your tutor and reply*

Masquelier, T.; Guyonneau, R. & Thorpe, S. J. (2008), 'Spike timing dependent plasticity finds the start of repeating patterns in continuous spike trains.', *PLoS ONE* **3**(1), e1377. (*model study*) [[leaky integrate and fire model neuron + Poisson process](#)]

Finelli LA, Haney S, Bazhenov M, Stopfer M, Sejnowski TJ. Synaptic learning rules and sparse coding in a model sensory system. *PLoS Comput Biol.* 2008 Apr 18;4(4):e1000062 . (*model study*) [[Hodkin Huxley type model neuron](#)]

III Coincident spiking in neural ensembles: The synfire chain hypothesis

[6 **Hannah Dold** ✓] *a + b (b is rather short and introduces dynamic correlation)*

Alonso, J. M.; Usrey, W. M. & Reid, R. C. (1996), 'Precisely correlated firing in cells of the lateral geniculate nucleus.', *Nature* **383**(6603), 815—819. [[cross correlogram](#)] (a)

Vaadia E, Haalman I, Abeles M, Bergman H, Prut Y, Slovin H, Aertsen A. (1995) Dynamics of neuronal interactions in monkey cortex in relation to behavioural events. *Nature.* 373(6514):515-8 [[joint PSTH](#)] (b)

[7 + 8 **Sven Dähne** ✓ + **Kai Görden** ✓] [Tutors: **Vinzenz Schönfelder + Farzad Farkhooi**]

Riehle, A.; Grün, S.; Diesmann, M. & Aertsen, A. (1997), 'Spike synchronization and rate modulation differentially involved in motor cortical function.', *Science* **278**(5345), 1950—1953. [[Unitary Event Analysis](#)]

+ *additional paper(s) on Unitary Event Analysis: Grün S, Diesmann M, Aertsen A. Unitary events in multiple single-neuron spiking activity: II. Nonstationary data. Neural Comput. 2002 Jan;14(1):81-119.*

[9 **Chris Häusler** ✓] [Tutor: **Denise Berger**] *please contact Denise Berger soon*

Maldonado, P.; Babul, C.; Singer, W.; Rodriguez, E.; Berger, D. & Grün, S. (2008), 'Synchronization of neuronal responses in primary visual cortex of monkeys viewing natural images.', *J Neurophysiol* **100**(3), 1523--1532. [[Unitary Event Analysis](#)]

IV Stimulus encoding by spike latency

⇒ *additional background reading on topic V*

Oram MW, Xiao D, Dritschel B, Payne KR (2002) The temporal resolution of neural codes: does response latency have a unique role? *Philos Trans R Soc Lond B Biol Sci.* 357(1424):987-1001

[10 **Martin Brill** ✓]

Thorpe, S.; Delorme, A. & Rullen, R. V. (2001) *Spike-based strategies for rapid processing.* *Neural Netw* **14**(6-7), 715--725.

[11 **Johannes Felsenberg** ✓]

Wesson, D. W.; Carey, R. M.; Verhagen, J. V. & Wachowiak, M. (2008) *Rapid encoding and perception of novel odors in the rat.* *PLoS Biol* **6**(4), e82.

[12 **Vinzenz Schönfelder** ✓]

Chase SM, Young ED (2006) *Spike-timing codes enhance the representation of multiple simultaneous sound-localization cues in the inferior colliculus.* *J Neurosci.* 26:3889-98

Reliability and Precision of Spike Generation in Cortical Cells

Jan Clemens

1 Introduction

For cortical cells to take part in a temporal code, they must themselves be able to transform temporally modulated inputs reliably and precisely into temporally patterned spike trains. For a long time it has been doubted that cortical neurons are able to generate such response patterns in a reproducible manner (see e.g. [Softky and Koch \(1993\)](#)).

Mainen and Sejnowski, in their 1995 paper titled “Reliability of Spike Timing in Neocortical Neurons”, provided unequivocal evidence that nerve cells are in principle able to take part in such a temporal coding scheme. Through current injections into cortical cells, they answered the following questions: How precisely can cortical cells translate synaptic input into spike trains? To what degree does precision depend on stimulus parameters?

2 Experiments and Methods

Preparation The temporal precision of pyramidal cells was quantified using noise current injections. Noise sources extrinsic to the neuron itself were eliminated by **1.** using a slice preparation, and **2.** pharmacologically blocking all remaining synaptic inputs. Current-clamped whole-cell recordings were performed.

Stimuli Temporally constant and modulated noise currents were injected via the recording electrode. Both stimulus types were calibrated as to evoke comparable mean firing rates between 10 and 25Hz. The dynamic noise stimulus was generated to mimic the dendritic integration of many independent excitatory and inhibitory synaptic inputs: Gaussian white noise was low pass filtered by convolution with an α function $\alpha(t, \tau) = t \exp(-t/\tau)$. The amplitude of stimulus fluctuations was adjusted through the noise variance σ^2 ; the time scale of the fluctuations was set by the filter’s width τ .

Measures The noise current injections produced sparse firing events, which were reproducible across different representations of the same stimulus. Events were detected by looking for peaks in the PSTH. *Reliability* was then quantified as the fraction of trials in which spikes occurred during such an event. The standard deviation of spike times in an event served as an estimate of *precision*. Furthermore, the time course of the average

current stimulus preceding a spike—the spike-triggered average—was calculated, to examine whether spikes are able to lock to characteristic patterns of synaptic input.

3 Results

1. **Constant amplitude stimuli evoked responses with reliable average firing rates but imprecise spike timing.** While the CV for both stimulus types was small (0.1 and 0.05 respectively), the spike patterns produced by the unmodulated stimulus exhibited a desynchronization over the time course of the stimulation: while the timing of the first few spikes after stimulus onset was reproducible across trials, a synchronized firing pattern was barely visible after as few as 5 spikes (see fig. 1 left).
2. **Temporally modulated stimuli evoked more reliable spike trains than unmodulated stimuli.** Overall precision of firing events under fluctuating stimulation ranged from .5-2ms, depending on the stimulus statistics. Spike time jitter was always much smaller than the average firing rate (25Hz, ISI 40ms) or the time scale of stimulus fluctuations ($\tau=3-25$ ms) (see fig. 1 right).
3. Faster and more strongly modulated current stimuli evoked more precise and reliable firing patterns.
4. **Action potentials were reproducibly evoked by specific input patterns.** The spike-triggered average stimulus is a positive transient in the input current, corresponding to the synchronous arrival of excitatory post-synaptic potentials.

4 Conclusions

The present study shows that naturalistic patterns of synaptic input are able to evoke reliable and precise spike patterns with (sub)millisecond precision when external noise sources are eliminated. This indicates that:

- Non-synaptic noise sources contribute only minimally to neuronal variability, rendering spike generation precise and reliable.
- Cortical cells are able to encode temporal patterns of synaptic input in spike patterns with high precision.

For the observed precision to be relevant for everyday neural computation, it is necessary for the synaptic input and for synaptic transmission to be reliable and precise, too. On this matter, there exists contrasting evidence: While some studies have found a high degree of variability in neurons fully embedded in a network (Shadlen and Newsome, 1998), there exists evidence that cortical neurons are able to exploit their potential to generate precise spike patterns from synaptic input (Fellous et al., 2004; Tiesinga et al., 2008). In addition, several studies have shown that this precise timing contains indeed stimulus-specific information (see e.g. Victor (1999)).

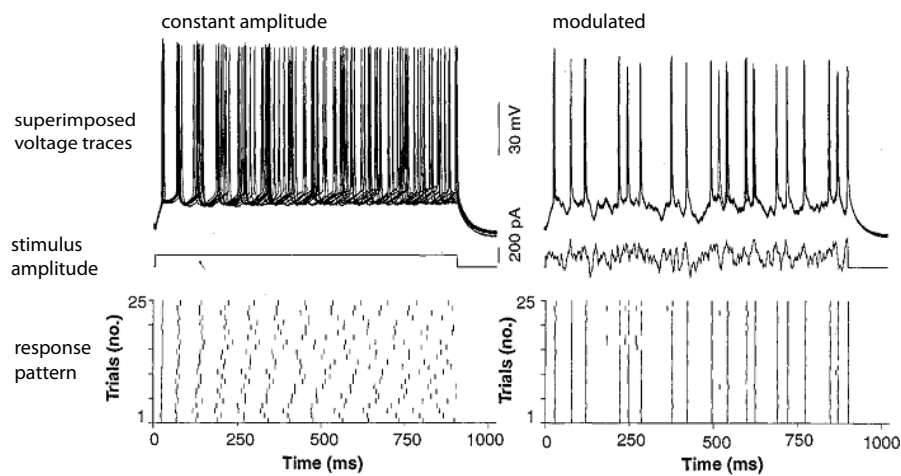


Figure 1: **Dependence of Neural Precision on Stimulus Type:** LEFT: Response patterns evoked by constant amplitude stimulation exhibit strong desynchronization of spike timing soon after stimulus onset. RIGHT: In contrast, the precision of spike timing during temporally modulated stimulation is maintained over the response's full time course. (modified after [Mainen and Sejnowski \(1995\)](#))

References

- J. M. Fellous, P. H. Tiesinga, P. J. Thomas, and T. J. Sejnowski. Discovering spike patterns in neuronal responses. *J Neurosci*, 24(12):2989–3001, 2004.
- Z. F. Mainen and T. J. Sejnowski. Reliability of spike timing in neocortical neurons. *Science*, 268(5216):1503–1506, 1995.
- M. N. Shadlen and W. T. Newsome. The variable discharge of cortical neurons: implications for connectivity, computation, and information coding. *J Neurosci*, 18(10):3870–3896, 1998.
- W. R. Softky and C. Koch. The highly irregular firing of cortical cells is inconsistent with temporal integration of random epsps. *J Neurosci*, 13(1):334–350, 1993.
- P. Tiesinga, J. Fellous, and T. Sejnowski. Regulation of spike timing in visual cortical circuits. *Nat Rev Neurosci*, 9:97–107, 2008.
- J. D. Victor. Temporal aspects of neural coding in the retina and lateral geniculate. *Network*, 10(4), 1999.

Synaptic modifications in cultured hippocampal neurons: Dependence on spike timing, synaptic strength, and postsynaptic cell type.

Guo-qiangu Bi and Mu-ming Poo

Recapitulation by Jakob Gutzmann

Synaptic efficacy is a highly dynamic cellular property which can be modified by physiological events like learning and memory, or by artificial stimuli. Commonly used protocols for the induction of synaptic modifications like Long-Term Potentiation (LTP) or Long-Term Depression (LTD) usually involve repetitive presynaptic stimulation and sometimes a constitutive postsynaptic polarization.

Basing their work on studies that had implicated the timing of a back-propagating action potential in the postsynaptic neuron with the depolarization elicited by the presynapse, the authors of the study presented here, Bi and Poo, attempted to fully characterize the dependency of synaptic modifications on the timing of pre- and postsynaptic action potentials. The Method and model they chose were Amphotericin B induced perforated patch recording on dissociated cultures of rat hippocampal neurons. A pre- and a postsynaptic neuron were patched and the nature of their connection was electrophysiologically and pharmacologically identified (Fig.1)

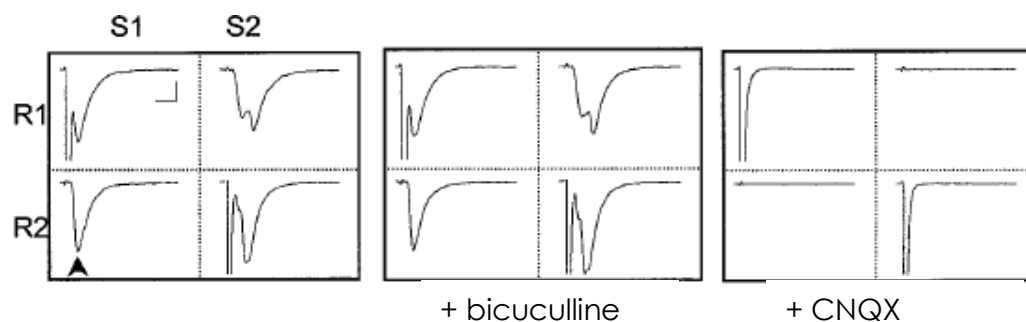


Figure 1: Sample recordings for two glutamatergic neurons (1 and 2). Matrices depicting EPSCs recorded from either neuron 1 (R1) or neuron 2 (R2), while either neuron 1 was stimulated (S1) or neuron 2 (S2). Arrowhead indicates a monosynaptic EPSC, which were focus of the study. Synaptic transmission was glutamatergic in nature, because the GABA receptor blocker bicuculline had no effect, but the AMPA receptor blocker CNQX inhibited transmission in both directions.

From each pair of neurons that the authors investigated, the baseline amplitude of monosynaptic EPSCs was measured by low frequency test stimuli (0,03 Hz, Clamp Voltage $V_c = -70\text{mV}$). Once the baseline was established, the authors switched the patch configuration to current clamp to allow both cells to spike and induced a series of 60 pulses at 1 Hz. If the EPSP was too weak to elicit an action potential in the postsynaptic neuron (subthreshold EPSP), the authors injected a spike inducing current into the postsynaptic neuron either after the EPSC (positively correlated postsynaptic spiking) or before the EPSC (negatively correlated postsynaptic spiking). After the repetitive stimulation cells were held in voltage clamp again and test stimuli were induced to determine EPSC amplitude. The authors could clearly show, that postsynaptic spiking positively correlated with the presynaptic stimulation led to an increase in mean EPSC amplitude and, vice versa, negatively correlated postsynaptic spiking led to a weakening of synaptic connectivity.

For all further experiments the authors only used subthreshold synaptic connections where they could induce a postsynaptic spike at a time of their choosing and thereby investigate the dependence of synaptic modification on spike timing. Figure 2 shows the critical time window which the authors concluded from their experiments. If the EPSP is elicited up to 20ms before the postsynaptic spike, the synaptic connection is strengthened. But if the EPSP is elicited up to 20ms after the postsynaptic spike, the synaptic connection is weakened.

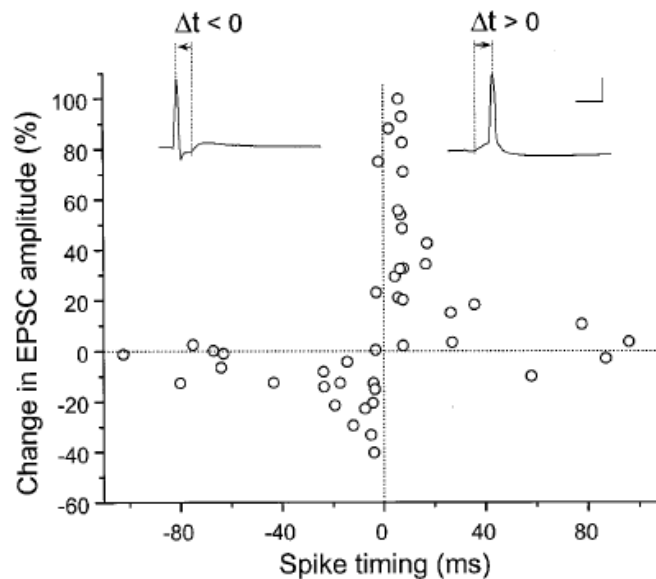


Figure 2: Critical time window for spike timing dependent plasticity. The percentage change in the EPSC amplitude before the correlated stimulation of pre- and postsynaptic neuron was plotted against the spike timing of the correlation. The spike timing (or Δt in the small graphics) is the time between the peak of the postsynaptic spike and the onset of the EPSP. Spike timing of -20ms to 0ms leads to synaptic depression and spike timing of 0ms to +20ms leads synaptic potentiation. Calibration for the small graphics: 50mV, 10ms

Apart from the major conclusion of this paper, that synaptic modification in cultured hippocampal neurons is dependent on the timing of pre- and postsynaptic spikes, the authors also investigated, which other factors may contribute to synaptic modifications. An important factor was revealed by the observation that the extend of synaptic potentiation, but not depression, is negatively correlated to the initial synaptic strength. Mostly synapses with initial EPSC amplitudes of 500pA or less could be potentiated by positively correlated spike timing.

Another factor influencing synaptic modification by spike timing is the postsynaptic celltype, because glutamatergic connections onto GABAergic neurons could neither be potentiated nor depressed by the authors. This may be due to the lack of the Ca^{2+} dependent enzymes CaMKII alpha and the phosphatase calcineurin, which have been shown to be lacking in this type of synaptic connections in the cortex and the hippocampus.

The last very interesting finding by the authors is the fact, that synaptic depression, induced by negatively correlated spike timing, is dependent on L-Type voltage gated Ca^{2+} -channels (LVGCC). Synaptic potentiation was reduced by the LVGCC-blocker nimodipine, but was not completely prevented, as was synaptic depression.

Summary to the seminar talk

”The tempotron: a neuron that learns spike timing-based decisions”

Felix Franke, Bernstein Center for Computational Neuroscience Berlin

08.02.2009

1 Introduction

Neurons retrieve spikes as their input. The question how they compute when to fire an output spike depending on their input, is a key question for computational neuroscience. Probably the most popular model for this computation is the integrate and fire neuron. However, one of the most common models for the computation of a neuron in machine learning is the perceptron which is strikingly different from the integrate and fire neuron. The paper [1] tries to close this gap and gives a possible learning rule for a classifier based on the integrate and fire neuron. The remainder of this article is organized as follow. In section 2 the key characteristics of the perceptron are briefly described. Then the integrate and fire neuron is reviewed in section 3 based on the recent work of [2]. Finally the Tempotron is introduced (section 4) and some of the interesting results are presented (section 5).

2 The Perceptron

Originally published in 1957 by Frank Rosenblatt [3], the perceptron has become one of the most influential machine learning algorithms. Due to its simplicity - it is completely linear - it is relatively easy to analyze and its learning rule is proven to converge. The input is a binary vector x , whose elements x_i indicate whether a spike arrived at the corresponding synapse i or not. All inputs are scaled with the respective weight w_i of every synapse and summed up (see eq. 1). If this sum is larger than a fixed threshold b , the neuron fires a spike i.e. the output $f(x)$ is 1 (see fig. 1 a).

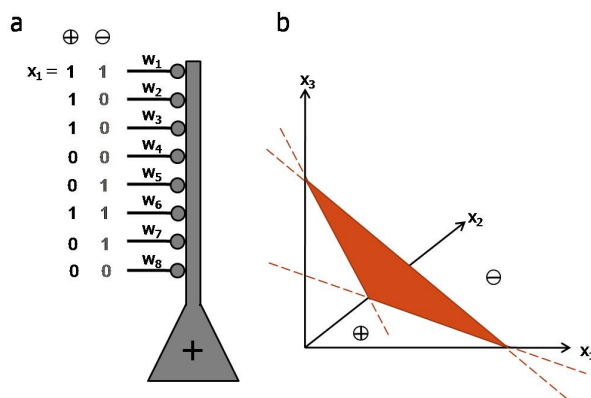


Figure 1: Schematic of the perceptron computation. **a** Each afferent of the perceptron receives a binary input (black and grey numbers correspond to a \oplus and \ominus stimulus, respectively). **b** Vector space representation of the linear classification as a hyperplane.

$$f(x) = \begin{cases} 1, & \text{if } w \cdot x + b > 0 \\ 0, & \text{else} \end{cases} \quad (1)$$

This computation equals a hyperplane as decision boundary in the input space (see fig. 1 b). Thus, the learning of the perceptron is equal to finding the normal vector of that plane. The offset is given by b .

3 The Integrate and Fire Neuron

The most prominent difference of the integrate and fire neuron to the perceptron is, that it has timeseries as its input or in the discrete case, a series of input vectors x . Here, every input spike causes a discrete change - the postsynaptic potential - in the intracellular voltage $V(t)$ of the neuron. The height of this change is different for every synapse, again scaled by ω_i . If the intracellular voltage reaches a threshold V_{thr} , the neuron fires a spike and the voltage is reset to V_{rest} . This means, the integrate and fire neuron integrates its inputs over time until it fires a spike. A common modification to the integrate and fire neuron is a leak. Here, the voltage also drops over time, depending on its momentary amplitude. This can easily be modeled by convolving the input spike trains with a certain kernel (see fig. 3 c) depending on the decay time of the membrane τ and the synaptic currents τ_s .

$$V(t) = \sum_i \omega_i \sum_{t_i} K(t - t_i) + V_{rest} \quad (2)$$

$$K(t - t_i) = V_0 \left(e^{-\frac{-(t-t_i)}{\tau}} - e^{-\frac{-(t-t_i)}{\tau_s}} \right) \quad (3)$$

Thus, every spike causes a change of the intracellular voltage depending on the time since the spike arrived at a synapse. The longer this time the smaller the influence of the spike. The factor V_0 is needed to normalize the kernel to amplitude 1, so that, again, only the synaptic weight vector ω influences the height of a postsynaptic potential.

4 The Tempotron

The task the Tempotron tries to solve is to learn a binary classifier for a given set of binary labeled input patterns based on the integrate and fire neuron described above. An input pattern consists of a series of spike times for every synapse. Or in other words, instead of a certain instantaneous spike configuration like in the case of the perceptron, the Tempotron receives a series of such configurations. Furthermore, the influence of this spikes on the intracellular voltage decreases over time. This is the same as convolving the inputs with a kernel before summing them up. Every pattern is classified as a \oplus stimulus

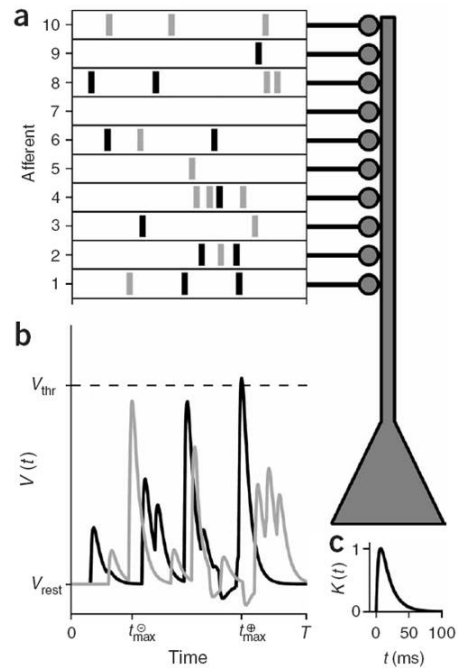


Figure 2: Schematic of the Tempotron computation. **a** Each afferent of the tempotron receives a spike train as its input (solid bars, black and grey bars correspond to \oplus and \ominus stimuli, respectively). **b** Voltage traces for the two input patterns from **a**. **c** Voltage trace for one input spike.

if at any point in a certain time T the intracellular voltage $V(t)$ reaches a threshold V_{thr} . The integration of the spikes is given by equations 2 and 3. The update equation for the synaptic weights can now be found by setting up an error function E . If a spike is elicited in a \ominus pattern, the maximal peak of the intracellular voltage trace at time t_{max} had to be above V_{thr} . Thus the error value is defined as the difference of the maximal peak to the threshold. Analogously if no spike is elicited for a \oplus trial then the maximal value of the voltage trace had to be below V_{thr} . Here, the error value will be the difference between the threshold and this maximal peak. This yields the error function

$$E_{\pm} = \pm(V_{thr} - V(t_{max}))\Theta(\pm(V_{thr} - V(t_{max}))) \quad (4)$$

for \oplus and \ominus patterns respectively and Θ being the Heavside step function. Differentiation of E in respect to the synaptic weights yields the update rule

$$\Delta\omega_i = \lambda \sum_{t_i < t_{max}} K(t_{max} - t_i) \quad (5)$$

with $\lambda > 0$ specifying the maximal change of the synaptic weight for every input spike. To sum up, the weight vector is only adapted if a pattern is erroneously classified. Then every synapse is updated for every spike it received before t_{max} . t_{max} is the time point of the erroneous output spike (\ominus patterns) or the maximal value of the voltage trace (\oplus patterns). The value of the update depends on the time between the input spike and t_{max} .

5 Results

The main results of the paper presented are:

- The Tempotron is able to successfully learn the weight vector for the binary classification task.
- The number of patterns that can be distinguished is approximately 3 per synapse (the so called load) subject on the exact parameterisation of the Tempotron.
- The load of the Tempotron is larger than that of a perceptron.
- The Tempotron is relatively robust to noise in the input patterns, however this robustness heavily depends on the load and other parameters.
- The Tempotron can learn to distinguish patterns based on higher order correlations.
- The update rule is not biologically plausible, since the time between every input spike and t_{max} has to be stored. However, the authors give a heuristic update rule which is more biologically plausible. The idea behind this heuristic is to update every synapse shortly after every input spike.

References

- [1] R. Gütig, H. Sompolinsky (2006), The tempotron: a neuron that learns spike timing-based decisions, *Nat Neurosci* 9:420-428154 (1-2) (2006) 204–224.
- [2] A.N. Burkitt (2006), A review of the integrate-and-fire neuron model: I. Homogeneous synaptic input. *Biol Cybern* DOI:10.1007/s00422-006-0068-6
- [3] Rosenblatt, Frank (1958), The Perceptron: A Probabilistic Model for Information Storage and Organization in the Brain, *Cornell Aeronautical Laboratory, Psychological Review*, v65, No. 6, pp. 386-408.

Modul II, Learning spike patterns: Spike Timing Dependent Plasticity & Tempotron

Vortrag 5, Jan-Ole Christian:

Masquelier T, Guyonneau R, Thorpe S (2008), 'Spike Timing Dependent Plasticity Finds the Start of Repeating Patterns in Continuous Spike Trains', PLoS ONE 3(1): e1377

Zusammenfassung

Masquelier [1] und Kollegen haben in einer Modellstudie gezeigt, dass mit *Spike Timing Dependent Plasticity* (STDP) ausgestattete Modellneuronen in der Lage sind, wiederkehrende Muster von Aktionspotentialen (*spike patterns*) auch ohne explizite Zeitreferenz, also ohne Angabe eines Startzeitpunktes, zu erkennen, selbst wenn diese Spike-Muster in einem Rauschen von Aktionspotentialen verborgen sind.

Einleitung

Über lange Zeit wurde angenommen, dass Neuronen Informationen ausschließlich durch einen Frequenzcode (also die Feuerrate von Aktionspotentialen) übermitteln. In den 1920er Jahren wurde in neurophysiologischen Studien von Adrian [3] gezeigt, dass die Feuerrate der Aktionspotentiale von Sinneszellen mit der Intensität eines Stimulus zunimmt.

Auch in künstlichen neuronalen Netzen (*artificial neural networks* ANN) wird die Feuerrate als Kodierungsschema benutzt. Sie gilt dabei als Maß für die Aktivierung eines Neurons. Der Aktivierungslevel eines Modellneurons wird den nachfolgenden Neuronen im ANN jedoch direkt als Wert übermittelt. Diese Verbindungen stellen das Äquivalent zu den Synapsen dar und sind in der Stärke ihres Einflusses (ihres Gewichts) auf das nachfolgende Neuron veränderlich. Die Aktivierung eines Modellneurons wird durch eine Funktion (zum Beispiel gewichtete Summe) der gemeldeten Eingaben an den Synapsen errechnet. Lernen findet in ANN durch das, nach Regeln erfolgende, Verändern der Gewichte statt.

Biologische Neuronen senden Informationen jedoch nicht als kontinuierlichen Wert, sondern als Sequenz von Aktionspotentialen. Für die Bestimmung der Feuerrate benötigt man mehrere Aktionspotentiale (also entweder einen längeren Zeitraum oder eine Population von gleichzeitig feuernenden Neuronen). Werden nun, um der biologischen Realität gerecht zu werden, statt eines kontinuierlichen Wertes die tatsächlichen Spikes simuliert, so werden Modelle, welche mit einem Frequenzcode arbeiten, sehr langsam und kompliziert. Diese Modelle können die Geschwindigkeit und Effizienz mancher beobachteten neuronalen Verarbeitung kaum erklären.

Dadurch, dass Neuronen Aktionspotentiale ausbilden, ergeben sich jedoch eine ganze Reihe von Spike basierten Kodierungsmöglichkeiten. Zum Beispiel, in welcher Reihenfolge Spikes von verschiedenen Afferenzen an den Synapsen ankommen. Ein prominentes biologisches Beispiel für solches Timing ist das auditorische System, in welchem ein Geräusch die beiden Ohren je nach Lage der Geräuschquelle zeitversetzt erreicht, so dass die entsprechenden Neuronen leicht zeitversetzt feuern. Und zwar in typischer Weise je nach Lage der Geräuschquelle. Aber auch der genaue Zeitpunkt oder die Synchronizität von Spikes eines räumlich-zeitlichen Spike-Musters können der Informationsübertragung dienen.

Elektrophysiologen bestätigen, dass in Neuronenpopulationen komplexe räumlich-zeitliche Spike-Muster auftreten, welche sich wiederholen. Diese Spike-Muster konnten sowohl *in vivo* als auch *in vitro* beobachtet werden.

Thorpe gibt in [4] einen Überblick über Spike basierte Kodierungsschemata und zeigt, dass Spike basierte Simulationen von asynchron feuernenden Neuronen ausgesprochen anspruchsvolle Aufgaben elegant und effizient lösen können.

In biologischen Neuronen kann sich die Stärke der synaptischen Übertragung in Abhängigkeit von der Aktivität der Synapse kurzzeitig oder dauerhaft ändern (synaptische Plastizität). Es handelt sich um Langzeit-Potenzierung (LTP Long-Term Potentiation), wenn der

Einfluss der Synapse dauerhaft verstärkt wird und umgekehrt bei einer dauerhaften Abschwächung des Einflusses der betroffenen Synapse um Langzeit-Depression (LTD Long-Term Depression).

In experimentellen Studien [2] wurde LTP beobachtet, wenn das präsynaptische Neuron kurz **vor** dem postsynaptischen Neuron gefeuert hatte. LTD konnte beobachtet werden, wenn das präsynaptische Neuron kurz **nach** dem postsynaptischen Neuron gefeuert hatte. Diese Erscheinung wird als *Spike Timing Dependent Plasticity* (STDP) bezeichnet. Dadurch wird das Gewicht jener Synapsen, die zu einem Aktionspotential beigetragen haben, verstärkt. Der Einfluss der Synapsen, die kurz *nach* einem ausgelösten Aktionspotential einen Input erhalten haben, wird dagegen abgeschwächt.

Diese Veränderung der synaptischen Gewichte ist um so stärker, je geringer der zeitliche Abstand des Inputs an der Synapse vom eigenen Aktionspotential ist. In computersimulierten Modellstudien kann die Stärke der Veränderung durch eine einfache exponentielle Update-Regel beschrieben werden, die gut mit den beobachteten Veränderungen übereinstimmt.

Wenn ein so modelliertes Neuron nun gleichartigen Salven von Input Spike-Mustern ausgesetzt wird, so hat dies zum Ergebnis, dass die synaptischen Gewichte für jene Afferenzen verstärkt werden, die in den Salven am frühesten feuern. Dies führt also dazu, dass schon die ersten eintreffenden Spikes ein Aktionspotential auslösen und die sich Reaktionszeit des Neurons auf die Salve verkürzt. In Messungen am Hippocampus von Ratten konnte in Übereinstimmung mit diesen theoretischen Betrachtungen gezeigt werden, dass die sogenannten 'place cells' früher feuern, wenn das Tier wiederholt ein entsprechendes Areal besucht hat [1].

In vielen Modellen wird jedoch vorausgesetzt, dass die Muster in Wellen auftreten, so dass leicht zwischen der Präsenz des Musters und Hintergrundaktivität unterschieden werden kann. Dies ist bei vielen biologischen Prozessen wohl tatsächlich der Fall. Zum Beispiel auch im visuellen System durch Sakkaden und Mikrosakkaden, im olfaktorischen System durch die Atemzüge beziehungsweise durch Schnüffeln. Außerdem verlangen viele Modelle, dass beim Lernen des Musters keine Distraktor-Wellen mit anderen Spike-Mustern auftreten.

Ergebnisse

Masquelier *et al.* [1] konnten ein Modell entwickeln, welches räumlich-zeitliche Spike-Muster auch dann erkennt, wenn diese

1. zu nicht vorhersagbaren Zeitpunkten auftreten,
2. wenn die Population der afferenten Neuronen mit innerhalb und außerhalb des Musters mit einer konstanten (gemittelten) Rate feuert,
3. wenn nur einige der afferenten Neuronen am Spike-Muster beteiligt sind.

Wenn sich also das Muster durch keine Charakteristika von der Hintergrundaktivität unterscheidet. Weder in der Feuerrate der gesamten Neuronenpopulation, noch in der Feuerrate der am Muster beteiligten Neuronen.

In der Computermodellierung wurden 2000 Neuronen über einen Zeitraum von 450 Sekunden simuliert. Die simulierten Neuronen feuerten nach einer Poisson Verteilung unabhängige Spike-Abfolgen (*spike trains*). Zu zufälligen Zeitpunkten verließen 1000 Neuronen gemeinsam den stochastischen Modus und feuerten für 50ms ein präzises Muster mit der gleichen Spike-Dichte. Außerdem erhöhten sie die Erkennungsschwierigkeit durch Hinzufügen einer Spontanaktivität zu allen Neuronen (auch während des Musters) und durch Hinzufügen einer Schwankung (Jitter) von einer Millisekunde, also durch Hinzufügen einer leichten Ungenauigkeit beim Timing.

In weiteren Simulationen wurden einige Parameter verändert, um deren Einfluss auf das Modell zu bestimmen.

Das unüberwachte Lernen des Musters geschah durch ein einziges *Leaky Integrate-and-Fire* (LIF) Neuron, welches von allen 2000 Afferenzen Input erhielt und als Koinzidenzdetektor fungierte.

Zu Beginn der Simulation waren alle synaptischen Gewichte gleich. Das LIF-Neuron war also nicht selektiv. Das präzise Muster hatte zunächst einen Anteil von etwa 1/4 der Gesamtzeit. Wegen der fast konstanten Spike-Dichte (gemittelt über die 2000 Neuronen) feuerte das LIF-

Neuron zu Beginn der Simulation periodisch mit konstanter Frequenz. Die anfängliche Feuerrate hängt von den Modellparametern Spike-Dichte, initiales Gewicht und Zeitkonstante der Membran ab.

Nach jedem ausgelösten Aktionspotential wurden die synaptischen Gewichte entsprechend der exponentiellen Update-Regel aktualisiert. In der Anfangsphase feuert das LIF Neuron sowohl innerhalb als auch außerhalb des zu erkennenden Spike-Musters. STDP führt durch Verstärkung und Abschwächung der einzelnen Synapsen zu einer Veränderung der synaptischen Gewichte, und zwar insgesamt zu einer Verringerung. Von den gewählten Parametern hängt ab, wie stark diese allgemeine Verringerung ausfällt. Das LIF-Neuron feuert im Verlaufe einer Simulation also seltener. Würde es gar kein sich wiederholendes Muster geben, so würde die Gewichte so weit verringert, dass gar kein Aktionspotential mehr ausgelöst werden würde. Da die am Muster beteiligten Afferenzen jedoch als einzige mehrmals gemeinsam verstärkt werden (da nur das Muster im zufälligen Rauschen mehrmals auftritt), erhöht sich die Wahrscheinlichkeit, dass das LIF Neuron innerhalb des Musters feuert. Es wird nach etwa 13,5 Sekunden selektiv für das Muster. Das ist sind etwa 70 Wiederholungen des Musters und etwa 700 Aktionspotentiale des LIF-Neurons.

Das LIF Neuron feuert anfangs zweimal pro Spike-Muster und es ist zufällig, auf welchen (zeitlichen und räumlichen) Teil des Musters es selektiv wird, welcher Spike-Anteil des Musters also initial verstärkt wird. Die steigende Selektivität führt jedoch schnell dazu, dass sich das LIF-Neuron lediglich einmal pro Muster entlädt.

Nachdem das LIF-Neuron selektiv geworden ist, führt die STDP dazu, dass jene Synapsen verstärkt werden, die kurz vor dem Auslösen des Aktionspotentials des LIF-Neurons einen Input erhielten. Dies sind ja nun die früheren Anteile des Musters. Es traversiert also im Verlaufe der Simulation durch das Spike-Muster zurück zu den ersten Spikes des Musters und feuert jedes mal etwas früher. Dies geschieht so lange, bis alle Synapsen, die an den ersten Spikes des Musters beteiligt sind, maximal verstärkt wurden. Die anderen Synapsen werden maximal unterdrückt. Die minimale Reaktionszeit tritt nach etwa 2000 Entladungen auf. Die postsynaptische Latenz beträgt dann etwa 4 ms. Die Trefferquote ist dann im Mittel 99.1% und es gibt keine Entladungen außerhalb des Patterns (keine *false alarms*). Nachdem das Lernen also stattgefunden hat, wartet das LIF-Neuron nur noch auf das gelernte Musters und feuert wenn es auftritt, aber nicht spontan. Es vergisst das Gelernte niemals.

Von den 2000 Synapsen sind in in der ersten Simulation 383 maximal verstärkt und der Rest fast vollständig unterdrückt.

Es wurden viele weitere Simulationen mit unterschiedlichen Mustern und variierten Parametern durchgeführt (Figure 7). Zunächst wurde der Anteil des Musters an der Gesamtzeit verringert. Dadurch reduzieren sich die Gewichte so weit, dass (bei einem steigenden Anteil der Simulationsdurchläufe) keine Entladungen mehr stattfinden, bevor das Muster gelernt werden kann. Dies entspricht dem Verhalten bei gar keinem wiederkehrenden Muster. Allerdings muss das Muster lediglich in der Lernphase häufig präsentiert werden. Ein gelerntes Muster kann danach sehr selten auftreten und führt doch zu einem Aktionspotential, während das LIF-Neuron sonst schweigt.

Ein weiterer Parameter, der variiert wurde, ist der Jitter. Die Performance des Modells ist sehr gut für einen Jitter von weniger als 3ms.

Außerdem wurde der Anteil der am Muster beteiligten Neuronen variiert. Bei einem Anteil von nur 1/3 waren die Simulation immer noch in der Hälfte aller Fälle erfolgreich. Die 2/3 nicht am Muster beteiligten Synapsen wurden durch die STDP vollständig unterdrückt.

Der vierte variierte Parameter ist das initiale Gewicht. Je größer die initialen Gewichte sind, desto besser wird das Muster gelernt, da es in der Anfangsphase mehr Entladungen gibt und es seltener vorkommt, dass alle Gewichte so weit verringert werden, bis gar kein Aktionspotential mehr auftritt bevor das Muster gelernt wurde.

Ein weiterer variiertes Parameter ist der Anteil von fehlenden Spikes im Muster. Die Erfolgsquote sinkt bei fehlenden Spikes. Aber selbst bei einer Rate von 10% fehlenden Spikes beträgt die Erfolgsquote noch 82%.

Schließlich wurde noch die Zeitkonstante der Membran variiert (10ms im Grundversuch).

Mit kleinerer Zeitkonstante wurde die Latenzzeit geringer, auf die Erkennungsleistung hatte dieser Parameter aber wenig Einfluss. Das LIF-Neuron konnte noch die ersten nahezu zeitgleichen Spikes des Musters integrieren und feuern. Bei längerer Zeitkonstante wurden mehr Spikes des Musters integriert und die Latenzzeit wurde länger.

Diskussion

Das vorgeschlagene Lernschema ist völlig unüberwacht. Das Muster wird ohne eine explizite Zeitreferenz gelernt. Die Variation der Parameter des Modells zeigt, dass es erstaunlich robust gegenüber Störungen ist. Das Modell wäre mit biologischer Hardware einfach zu implementieren und es wäre verwunderlich, wenn dieser Mechanismus nicht auch in der Evolution entstanden sein sollte.

Bisherige Modelle funktionierten lediglich mit Wellen von Spike-Mustern. Dieses Modell kann auch Muster von einer Hintergrundaktivität unterscheiden, wenn die stochastischen Charakteristika von Muster und Hintergrundaktivität gleich sind.

Die Reaktionszeit auf das Muster verringert sich im Verlaufe der Simulation bis es einen minimalen stabilen Wert erreicht hat. Dies geschieht durch die Konzentration der Gewichte auf die Afferenzen, welche als erste im Muster feuern.

Eine Limitierung mag sein, dass es nur exzitatorischen Einfluss der Synapsen gibt. Muster in denen eine bestimmte Afferenz **nicht** feuern darf, können vom Modell nicht gelernt werden. Wenn mehrere Spike-Patterns präsentiert werden, wird das Modell nur eines davon lernen. Der Zufall wird bestimmen welches.

Im Spike-Muster wird das fast zeitgleiche Auftreten von Spikes gelernt. Das gesamte räumlich-zeitliche Muster wird nicht einbezogen. Insbesondere das Timing innerhalb des Musters ist nicht von Bedeutung. Das Modell wäre nicht in der Lage, Regeln zu lernen, in welchen nur das Timing eine Rolle spielt, also zum Beispiel: „Das LIF-Neuron feuert wenn die Afferenzen 1-500 nacheinander feuern und sonst nicht.“

Doch dann gäbe es ja kein festes Muster mehr und es sollte ja zunächst nur gezeigt werden, das ein mit STDP ausgestattetes LIF-Neuron sehr zuverlässig ein festes zeitlich-räumliches Muster lernen und mit minimaler Latenzzeit reagieren kann.

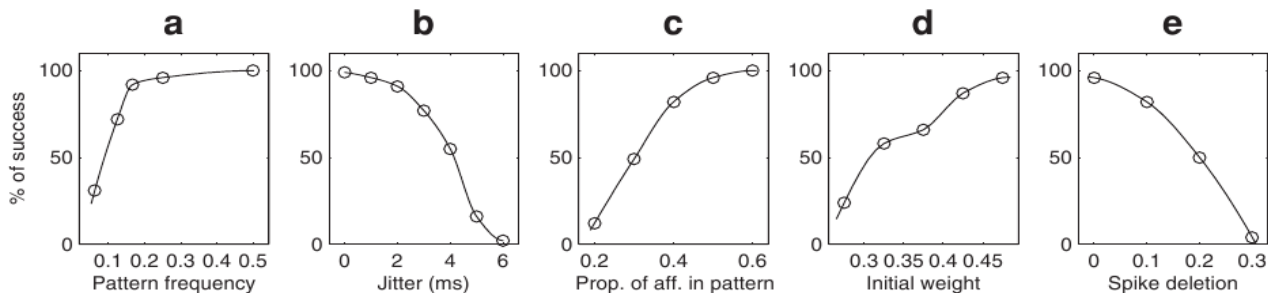


Figure 7. Resistance to degradations (100 trials). (a) Percentage of successful trials as a function of the pattern frequency (pattern duration/the total duration, given a fixed pattern length of 50 ms). The pattern needs to be consistently present, at least at the beginning, for the STDP to start the learning process. (b) Percentage of successful trials as a function of jitter. For jitter greater than 3 ms spike coincidences are lost and the STDP weight updates are inaccurate, so the learning is impaired (c) Percentage of successful trials as a function of the proportion of afferents involved in the pattern. Performance is good if this proportion is above 1/3 (d) Percentage of successful trials as a function of the initial weights. With a high value the neuron can handle more discharges outside the pattern. (e) Percentage of successful trials as a function of the proportion of spikes deleted. With a 10% deletion the pattern was correctly learnt in 82% of the cases. doi:10.1371/journal.pone.0001377.g007

Literaturverweise

1. Masquelier T, Guyonneau R, Thorpe SJ (2008) Spike Timing Dependent Plasticity Finds the Start of Repeating Patterns in Continuous Spike Trains. PLoS ONE 3(1): e1377. doi:10.1371/journal.pone.0001377
2. Song S, Miller KD, Abbott LF (2000) Competitive Hebbian learning through spike-timing-dependent plasticity. Nat Neurosci 3: 919-926
3. Adrian ED (1928) The basis of sensation, New York: Norton.
4. Thorpe S, Delorme A, Van Rullen R (2001) Spike-based Strategies for rapid processing. Neural Networks 14: 715-725

SUMMARY

HANNAH DOLD

08/02/2009

J.-M. ALONSO, W. M. USREY AND R. C. REID¹

Precisely correlated firing in cells of the lateral geniculate nucleus

Possible hypotheses

If the correlated firing of neurons is functionally meaningful, then neurons with similar receptive fields should be stronger correlated than others.

If correlated thalamic neurons are more effective in driving a common cortical target than non-correlated neurons, then the peak of correlations between cortical cells spike trains with exclusively synchronous spikes should be higher than with non-synchronous spikes.

Methods

Nearby geniculate cells and cortical cells were simultaneously recorded in anesthetized and paralyzed cats. Receptive fields (RF) were calculated by reverse correlation using white-noise stimuli and a 52 Hz update rate. Subsequently cells were classified into on-center and off-center cells. For the first part of the analysis, cross-correlation analysis was performed on spike trains of LGN cell pairs.

To investigate the second hypothesis, correlations between two LGN cells and a cortical simple cell were computed separately for each LGN cell to indicate monosynaptic connections. In addition, the spikes of the LGN cells were divided into two classes. The first class contains spikes of one cell that occurred within a 1 ms interval of a spike in the second cell. The remaining spikes were assigned to a second class. Cross-correlations between the cortical cell and each class were computed. Furthermore, co-stimulation artifacts between cells were estimated with the shuffled correlogram. Efficacy is calculated as the percentage of thalamic spikes followed by cortical spike after removing stimulus dependent correlations.

¹ J.-M. Alonso, W. M. Usrey, and R. C. Reid. Precisely correlated firing in cells of the lateral geniculate nucleus. *Nature*, 383:815–819, 1996.

Cross-correlation
For two time-discrete and real-valued functions f and g the cross-correlation is defined by:

$$(f * g)[n] = \sum_{m=-\infty}^{\infty} f[m]g[n+m] \quad (1)$$

(adapted from <http://en.wikipedia.org/wiki/Cross-correlation/>)

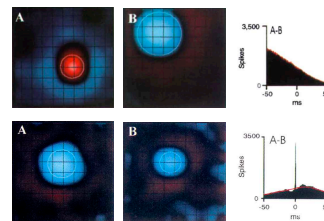


Figure 1: Upper row: The cross-correlogram of an off-center and an on-center cell with different receptive field positions does not exceed the shuffled correlogram (red line). Lower row: Two on-center cells with similar receptive fields show a pronounced peak in their cross-correlogram.

Results

Cross-correlation analysis on pairs of geniculate cells showed trends depending on the receptive field overlap of the cells. LGN cell pairs with non-overlapping RFs didn't show positive correlation, while 17 per cent of the pairs with partially overlapping RFs showed a positive correlation with a modulation strength of 1.9%. A correlation was observed in 48% of pairs with overlapping fields having the same sign with a strength of 10%. 79% of the pairs that additionally had a similar RF size were correlated with a strength of 13%. The maximal strength of 28% and 100% positive correlation was observed in cell pairs with overlapping RF of similar size, timing and sign. Figure 1 shows two examples of LGN cell pairs and the corresponding cross-correlograms.

Thirteen cases of geniculate cells pairs projecting to a common cortical cell were studied. Two cases contained LGN cells with overlapping RFs showing correlated firing, while no correlations were found for the LGN cells in the remaining nine cases. In 11 cases the efficacies of simultaneous spikes were significantly greater than the summed efficacies of non-simultaneous spikes. Figure 2 shows data from the uncorrelated LGN cell pair in Fig 1 and a cortical cell. The first correlogram contains only simultaneous spikes and the second only non-simultaneous spikes.

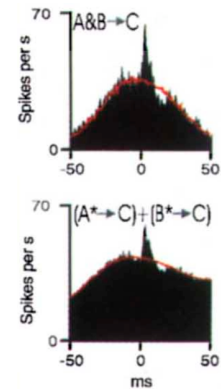


Figure 2: Correlation of spikes from cell A and B (Figure 1, lower row) with a cortical simple cell only containing simultaneous spikes ($A \& B$) or non-simultaneous spikes ($A^* + B^*$)

Conclusion

Strong correlations between geniculate cells were only observed for cells with similar receptive fields with respect to overlap, sign, size and timing. An increased efficacy of cortical target cells was observed for simultaneous spikes of correlated input neurons and for random simultaneous spikes of uncorrelated input neurons. The authors therefore suggest that the firing of tightly correlated LGN neurons could strengthen the thalamic input to a cortical simple cell by increasing the likelihood of synchronous spikes.

E. VAADIA, I. HAALMAN, M. ABELES, H. BERGMAN, Y. PRUT ,
H. SLOVIN, A. AERTSEN ²

Dynamics of neuronal interactions in monkey cortex in relation to behavioural events

Possible hypotheses

If the firing rates of neurons do not vary for different stimulus or behavioral conditions, then they could code different conditions by correlating their firing patterns with other neurons.

If neurons are grouped into functional units by correlation, then neurons from different groups should be less likely to be correlated than neurons within one group.

Methods

Two monkeys were trained to hold a central key. The trial starts with a ready signal (central red light) followed after 3 to 6 seconds by one of two spatial cues depicting the future correct response. The monkey had to postpone the response until a delayed trigger signal indicated to respond. In "Go" trials the monkey was supposed to touch the correct target. In "No-Go" trials monkeys were rewarded for not responding to the trigger signal and thus not releasing the central key.

The activity of 6-16 frontal cortex neurons was recorded simultaneously from the behaving monkeys. Additionally eye movements were monitored. The electrodes' positions were reconstructed from histological inspections. Cell pairs were analyzed using dynamic cross-correlation (joint peri-stimulus time histogram, JPSTH ³) to reveal the time structure of correlated firing with respect to either the stimulus or movements. All JPSTHs were corrected for stimulus or motion artifacts. The maximum of the coincidence-time histogram expressed as percentage of its expected rate is called the "maximal modulation depth".

Results

Separate JPSTHs for "Go" and "NoGo" trials of two premotor neurons are reported using a time interval around the ready signal. Neither the neurons' firing rates nor the conventional cross-correlogram differ for the two behavioral paradigms. However, the coincidence-time histogram shows modulations around the ready signal. In case of the "Go" task the co-firing is maximal after the ready signal. In contrary, co-firing drops to zero at about the same time in the "No-Go" condition (see Figure 4).

² E. Vaadia, I. Haalman, M. Abeles, H. Bergman, Y. Prut, H. Slovin, and A. Aertsen. Dynamics of neuronal interactions in monkey cortex in relation to behavioural events. *Nature*, 373:515-518, 1995.

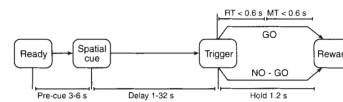


Figure 3: Flow diagram of the behavioral task

³ Kyle Kirkland. URL <http://mulab.physiol.upenn.edu/jpst.html>.

The same analysis was performed for two neighboring neurons and two distant neurons in relation to saccade onset and discriminating between leftward and rightward saccades. The average correlation increased (neighbors) or decreased (distant) during the saccade, whereas the firing rates of all neurons increased regardless of saccade direction. For the neighboring pair the coincidence-time histogram revealed that for a rightward saccade co-firing increases, while it falls for a leftward saccade. A negative correlation is observed between distant neurons after saccade onset to the right, whereas correlation is slightly positive after leftward saccade onset.

Correlated activity was found in 499 of 947 neuronal pairs and 61% of those correlated pairs showed fast changes in co-firing with respect to behavior. Furthermore, 83% of neighboring neurons (recorded by the same electrode) are positively cross-correlated around zero and the remaining 17% show a peak and a trough in the vicinity of zero ("compound correlation"). For distant pairs (recorded by different electrodes) the interval around zero shows positive sign in only 44% of the cases, negative sign in 20% and compound correlations are observed in the remaining 36%.

Conclusion

The authors advocate the following idea based on their results from dynamic cross-correlation: "A single neurons can intermittently participate in different computations by rapidly changing its coupling to other neurons, without associated changes in firing rate"⁴. They also propose that the trend between neighboring neurons to be positively correlated might indicate that the former tend to be activated collectively forming a temporary functional group. Negative correlations for distant neurons could denote that they belong to a different group and are thereby clearly discriminable.

References

J.-M. Alonso, W. M. Usrey, and R. C. Reid. Precisely correlated firing in cells of the lateral geniculate nucleus. *Nature*, 383: 815–819, 1996.

Kyle Kirkland. URL <http://mulab.physiol.upenn.edu/jpst.html>.

E. Vaadia, I. Haalman, M. Abeles, H. Bergman, Y. Prut, H. Slovin, and A. Aertsen. Dynamics of neuronal interactions in monkey cortex in relation to havioural events. *Nature*, 373:515–518, 1995.

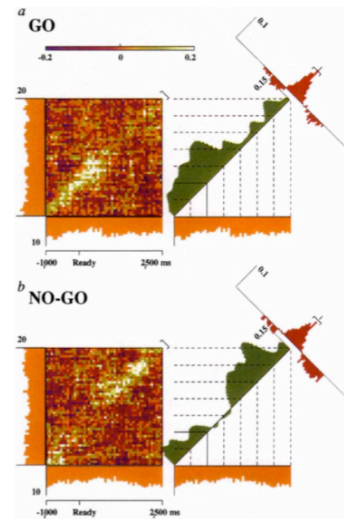


Figure 4: JPSTH for two neurons divided into "Go" and "NoGo" conditions

⁴ E. Vaadia, I. Haalman, M. Abeles, H. Bergman, Y. Prut, H. Slovin, and A. Aertsen. Dynamics of neuronal interactions in monkey cortex in relation to havioural events. *Nature*, 373:515–518, 1995.

Detecting Coincident Firing with Unitary Event Analysis

Sven Dähne, Kai Görden

Bernstein Center for Computational Neuroscience, Berlin

February 10, 2009

Abstract

The detection of temporal codes in neuronal populations requires methods that allow for a reliable identification of synchronous events. In this report we describe the work of Riehle et al [10] who have invented a method called Unitary Event Analysis (UEA) which detects epochs of excessive firing coincidences. We explain the method and its underlying assumptions and describe how Riehle et al applied it to investigate the functional role of spike synchronization versus rate modulation. We conclude with brief critical discussion of this method.

1 Introduction

The question of how information is represented and processed in human or animal brains lies at the very heart of neuroscience. It seems obvious that neuronal discharges, or action potentials (APs), play a major role in information processing. They provide neurons with the means of communication which is an essential ingredient in any information processing apparatus. However, to the present day it is an open question how exactly neurons use their spiking ability to represent information.

Two major theories have been proposed and supported by experimental evidence which suggest mechanisms of how the brain encodes information: rate coding and temporal coding. Rate code approaches postulate that the brain uses the number of APs per unit time to convey information. It has been shown, that by assuming the brain uses a rate code, it is possible to decode internal states as well as external stimuli. The rate code hypothesis is, for example, supported by Georgopoulos et al [6]. They were able to predict the arm movement of a monkey merely by observing the firing rates of a population of neurons in motor cortex. Investigating sensory coding in the visual system rather than executive motor functions, Warland et al [15] were able to decode presented visual input from the output of retinal ganglion cells by applying a linear operator to an estimate of the firing rate. This suggests that the firing rate of the ganglion cells carried the necessary information.

Temporal codes, on the other hand, assume that it is the timing aspects of APs, e.g. time or phase locking, which convey information and aids in processing. A prominent example of this class of coding strategies is the binding-by-synchrony hypothesis (see [3] for a review), brought forward by Wolf Singer and colleagues. This theory tries to explain how spatially segregated computations can be bound together to cause coherent perceptions or actions, and information in a network can be routed. Based on these and other findings, Pascal Fries more recently put forward the Communication-Through-Coherence hypothesis, in which he argues that neuronal assemblies use massive synchronous firing to communicate the results of neuronal computations within these assemblies to other assemblies, using spatial summation to trigger action potential generation at the postsynaptic cells [5]. For reviews on other studies that support temporal coding see [11] and [14].

The debate between supporters of the two coding schemes is a lively one. For example, see [12] for a rather critical discussion of temporal coding approaches and their empirical support.

A study by Alexa Riehle et al [10] focuses on the motor domain and investigates how aspects of both major coding strategies (spike rate modulation and spike synchrony, specifically coincidental firing of neuron pairs) can be involved in cortical control of executive motor functions. In this report we will describe the experimental setup and analysis methods used in the study by Riehle and co-workers. We will then proceed and report their findings. In the final part we will discuss possible weaknesses of the method and relate the conclusions they have drawn from their results to those of other studies.

2 Methods

2.1 Experimental Setup

In their study, Riehle et al presented their subjects (two macaque monkeys) with a delayed match to sample task, while recording extra-cellularly from motor cortex with a multi electrode setting. In each trial, the monkey was shown two visual stimuli, separated by a waiting period of a certain duration, called the preparatory period (PP). The first, or preparatory, signal (PS) indicated a target position to which the monkey was trained to point with a lever once the second signal (response signal, RS) was shown. A trial was considered to be performed correctly, if the monkey had waited during the PP for the RS to appear and then pointed to the location previously indicated by the PS. The PP was always one of four predefined lengths and was chosen randomly from that set for each trial. Figure 1 (A) illustrates the possible time courses for a single trial and the order of the described signals. It is important to note, that by choosing the length of the PP from four possible durations only, the monkeys are able to learn these durations and anticipate the occurrence of the RS. This effect is visualized in figure 1 (B). The response times for trials with a longer PP are shorter, because the longer it takes for the RS to appear, the more likely is one of the longer PP.

2.2 Unitary Event Analysis

A key aspect of the analysis is the detection of the so-called *unitary events* ([7]). The underlying idea is to calculate the probability that the empirically found number of certain coincidence patterns is caused by chance, given that the different cells fire independently of each other. To test for this, Grün et al developed a statistical measure which they call *joint surprise*. The measure is calculated like follows: After spike detection and spike sorting, the spike trains of a certain time interval of length \mathcal{T} are binned in a binary vector $\mathbf{v}(t)$ with T bins of length Δ (see figure 1 (C)) according to

$$(2.1\&2.2)^1 \mathbf{v}(t) = \begin{bmatrix} v_1(t) \\ \vdots \\ v_i(t) \\ \vdots \\ v_n(t) \end{bmatrix}, v_i(t) = \begin{cases} 1, & \text{if spike in } [t, t + \Delta) \\ 0, & \text{if no spike in } [t, t + \Delta) \end{cases}$$

$$t = 0, \dots, (T - 1) \cdot \Delta; i = 1, \dots, N; v_i \in \{0, 1\}.$$

Thus, the resulting vector for the t^{th} bin $\mathbf{v}(t)$ contains as elements for each of the N recording channels either a 0, if no spike was recorded in the time period for that channel, or a 1, if at least 1 spike (or more) were recorded. As each vector $\mathbf{v}(t)$ is a binary representation of N channels (that is, it contains a combination of N 0s and 1s, there are $m = 2^N$ possible different $\mathbf{v}(t)$.

To enumerate all these different combinations, in the following the vector \mathbf{v}^k will identify the vector containing the k^{th} pattern (v_N^k, \dots, v_1^k) , where k is the

¹All equations are taken from and numbered as in [7]

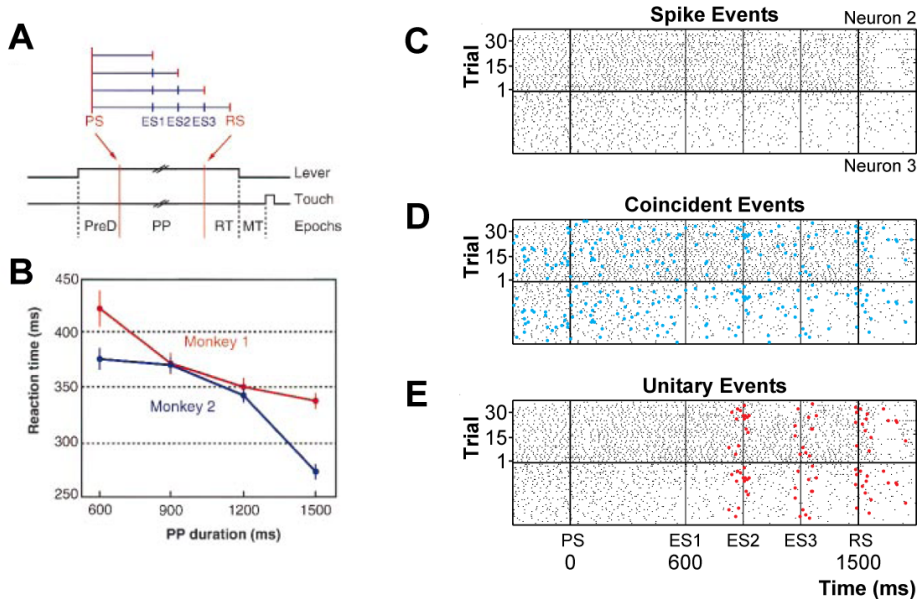


Figure 1: (A) Time course of the experiment. See Section 2.1 for details. (B) Reaction times of the monkeys plotted against the duration of the preparatory period (PP). (C-E) Steps of the data analysis. The three raster plots show the same data (2 neurons, 36 trials with longest PP) after the processing steps of UEA. (C) Spike train data, with trials on the y axis and time on the x axis. (D) Same as in (C), with blue dots marking the detected coincident spikes. (E) Same as in (C), with red dots marking unitary events (UEs), i.e. coincident spikes in regions where the coincident rate is significantly larger than expected by chance. These regions are called UE epochs.

binary interpretation of $\mathbf{v}^k + 1$, i.e. $k = (v_N^k \dots v_1^k)_2 + 1$.² n_k will denote the empirical number of observations for each of these specific patterns \mathbf{v}^k .

For each \mathbf{v}^k , the probability $P(\mathbf{v}^k)$ of observing it under the Null-Hypothesis that all channels fire independently can be calculated by multiplying the individual probabilities $p_i = P(v_i = 1)$, if a spike occurred in channel i , or $1 - p_i = P(v_i = 0)$, if no spike occurred in channel i :

$$(2.3) H_0 : P_k = P(\mathbf{v}^k) = \prod_{i=1}^N P(v_i^k), \text{ with } P(v_i^k) = \begin{cases} P(v_i = 1), & \text{if } v_i^k = 1 \\ 1 - P(v_i = 1), & \text{if } v_i^k = 0 \end{cases}$$

To estimate p_i , Grün et al chose the frequency interpretation of firing rates, according to which number of observed spike events c_i occurring during the time period T is distributed randomly over the T considered time bins, and hence $p_i = c_i/T$.

Using the assumption that each binned recording vector v_i describes a Bernoulli trial (i.e. that the occurrence of a spike in one bin does not depend on a possible occurrences in the bins before, or more formally $p(v_i(t)|v_i(t-1)) = p(v_i(t))$,

²For example, $\mathbf{v}^1 = (0, \dots, 0, 0)$ identifies the vector without any spike events, as $(0 \dots 0)_2 + 1 = 1$, $\mathbf{v}^2 = (0, \dots, 0, 1)$ the vector for which a spiking event occurred only in channel 1, and so on.

[4]), and using limit properties to further transform the resulting Binomial distribution into a Poisson distribution, Grün et al derive a formula to calculate the probability $\psi(n_k; P_k; T)$ that a pattern \mathbf{v}^k with the probability P_k occurs exactly n_k times during T bins, which is given by

$$(2.8) \psi(n_k; P_k; T) = \frac{(P_k \cdot T)^{n_k}}{n_k!} \cdot \exp(-P_k \cdot T), k = 1, \dots, m.$$

As the expectation of the Poisson formula is well known, it follows that the number of predicted occurrences n_k^{pred} for each pattern v_k is given by $n_k^{pred} = \langle \psi \rangle = P_k \cdot T$. In order to calculate the statistical significance of deviation for a specific pattern \mathbf{v}^k from H_0 (i.e. from independent firing between channels), the probability $\Psi(n_k^{emp} | n_k^{pred})$ to find the empirical observed number of occurrences n_k^{emp} or more given H_0 can be calculated like

$$(2.9) \Psi(n_k^{emp} | n_k^{pred}) = \sum_{n_k=n_k^{emp}}^T \psi(n_k, n_k^{pred}) = \sum_{n_k=n_k^{emp}}^T \frac{(n_k^{pred})^{n_k}}{n_k!} \cdot \exp(-n_k^{pred}).$$

Although in their Science paper [10] Riehle et al only consider significantly large numbers of observations and mainly describe pairs of channels, the described test in principle allows to test for simultaneous spike events in multiple channels (e.g. [7]) or for significantly few observations as well.

As the interesting values for Ψ are all very small, Grün et al. chose to enhance the visual resolution by applying the following transformation which they call the *joint-surprise* measure $S(\Psi)$

$$(2.10) S(\Psi) = \log \frac{1 - \Psi}{\Psi}.$$

Using the *joint-surprise* measure, all those patterns \mathbf{v}^k are labeled unitary events, for which the calculated *joint-surprise* value S_k is larger than some predefined threshold S_α (for example $S_{\alpha=0.01} = 2$ for a statistical $\alpha = 0.01$). Remember that this test has to be calculated separately for each pattern of interest v_k .

Up to here, it has been assumed that within the time range \mathcal{T} the firing rates would be stationary. However, this is obviously not the case for normal experiments. In order to overcome this problem, Grün et al suggest to use 2 tricks [8]: First, to use a sliding window of relative short length and then to calculate the firing rate estimations p_i and the *joint-surprise* value S_k every time. They argue that during such a short time window the firing rates can be assumed to be quasi-stationary. This, however, leads to relatively few data. To compensate for this, the proposed second trick is to pool data over multiple trials, assuming that the rates are constant if all data is time locked to a certain event within a trial.

3 Results

After having explained the data acquisition as well as one important data analysis method (UEA) in the previous section, we will now summarize Riehle et al's findings.

Figure 3 displays the main results of Riehle et al’s study. First of all, the UE epochs seemed to be aligned with the four possible time points at which the response signal could appear. Also, the pairs of synchronous firing changed for different UE epochs, reflecting dynamically changing synchrony networks.

When furthermore comparing the rate of coincident spikes in UE epochs, the authors found that the coincident rate was larger in epochs associated with longer PPs. This suggested that UE epochs, i.e. synchronization of firing, covary not only with the timing of an expectation but also with the degree of certainty (see figure 3 (A, B)). Sorting trials according to behavioral aspects revealed a correlation with these factors as well. Figure 3 (A) shows that trials with faster reaction times (RT) exhibit a larger number and more clearly pronounced UE epochs as opposed to trials in which the monkey took longer to react. The difference in UE abundance is even more obvious when correct trials are compared to trials in which the monkey did not respond (figure 3 (B)).

In a next step Riehle et al investigated the change, or modulation, of individual neuron’s firing rates within Unitary Event epochs. In order to quantify the rate modulation, they computed the time dependent *activity modulation index* (AMI) within UE epochs. Figure 3 (C) depicts AMI histograms of trials in which visual signals (PS or RS) are actually shown and of trials in which the signals are merely expected. In the signal-occurred conditions the distributions have more mass for larger values of the AMI. A threshold on AMI value scale was determined to classify pairs of neurons as either exhibiting rate modulation or not exhibiting rate modulation in the respective UE epoch. Figure 3 (D) depicts the total number of UE pairs sorted according to stimulus-expected versus stimulus-occurred condition. This plot also shows how many of the pairs exhibit rate modulation (yellow part of the bar). The total number of UE pairs is moderately larger in the stimulus-occurred condition. However, there are much more pairs which show rate modulation in the stimulus-occurred condition.

4 Discussion

In this section, we briefly discuss a few of the assumptions that underly the method of unitary event analysis and also relate the findings of Riehle et al to those of other studies.

Unitary Events are defined as the coincidental firing of two or more neurons. However, the term coincidental is not to be taken literally, as the coincidence time window used by Riehle et al was 5 ms long. Considering that a single action potential lasts between 2 and 3 ms [2], a 5 ms time window allows spike pairs to become marked coincident although the individual spikes were actually successive. Riehle et al could argue, that for neurons with large dendritic arbors, action potentials arriving in succession of a few milliseconds at distant dendrites may lead to postsynaptic potentials which reach the soma in shorter succession or even at the same time. Then the postsynaptic currents would reach the soma simultaneously and have an additive effect. So for the postsynaptic cell these successively arriving APs would appear to be coincident. In that situation, a longer time window than action potential duration would indeed be justified. However, there will always be false positives³ among the coincident events, and

³Successive spikes that get marked as coincident spikes.

the number of those increases with time window width. For a detailed analysis of the effects of time window length see [7].

In order to deal with rates that are non-stationary within trials, the algorithm assumes that the rate of neural responses to the same stimulus conditions are stationary within a small time window over trials. However, the authors of [1] report considerable variability of neural as well as behavioral responses the same stimuli over trials, which casts doubt on the stationarity-over-trials assumption, especially if the time window is very small. Another important assumption of the algorithm is that the neuron's response follows a Poisson distribution. The Poisson model for spike trains seems to be well accepted in the theoretical neuroscience community [2], but there are also studies which question its validity [13]. Since the UE algorithm is based on assumptions about neural firing whose validity is not entirely established and a larger coincident time window is more susceptible to false positives, the results of the algorithm have to be considered with some caution. In order to increase the trustworthiness of the results, we suggest to test the mentioned assumptions (stationarity-over-trials and Poisson-distributed-response) in ones data before applying the UE algorithm and to use a time window which is more in the range of action potential duration.

What should one make of the UEs after they have been identified? Riele et al concluded that they play a functional role in planning and execution of voluntary movements, suggesting that they carry a considerable amount of information. Here it interesting to point out a study by Nirenberg and others [9], in which the authors investigated the information theoretic aspects of a time code mechanism. In their study they used the ganglion cells from the mouse retina and stimulated it with natural movies. In a first step they also identified neuron pairs with a correlation above chance. Then they measured the amount of information that these pairs carried about the presented stimulus given a specific encoding scheme. The interesting result was, that when a decoding strategy was employed that took correlations between cells into account, decoding performance was only 10% better than a decoding strategy that treated the cells as independent encoders. Hence, their results suggest that UE events (at least in the early visual system) may not play a great role in information processing.

As for the debate between temporal and rate coding approaches, the study of Riehle et al identified important roles for both mechanisms. They were able to show that for the processing of external stimuli neurons synchronize their firing as well as modulate their firing rates, whereas for processing of internal events synchronization (without rate modulation) seems to be the preferred mechanism. Their findings suggest that the brain employs both coding mechanism but uses them for different, possible distinct, purposes.

References

- [1] A. Arieli, A. Sterkin, A. Grinvald, and A. Aertsen. Dynamics of Ongoing Activity: Explanation of the Large Variability in Evoked Cortical Responses. *Science*, 273(5283):1868, 1996.
- [2] P. Dayan and L.F. Abbott. *Theoretical neuroscience*. MIT Press Cambridge, Mass, 2001.

- [3] A.K. Engel, P. Fries, W. Singer, et al. Dynamic predictions: oscillations and synchrony in top-down processing. *Nature Reviews Neuroscience*, 2(10):704–716, 2001.
- [4] W. Feller. An introduction to probability theory and its applications. vol. 1. 1968.
- [5] P. Fries. A mechanism for cognitive dynamics: neuronal communication through neuronal coherence. *Trends in Cognitive Sciences*, 9(10):474–480, 2005.
- [6] AP Georgopoulos, JF Kalaska, R Caminiti, and JT Massey. On the relations between the direction of two-dimensional arm movements and cell discharge in primate motor cortex. *Journal of Neuroscience*, 2:1527–1537, 1982.
- [7] Sonja Grün, Markus Diesmann, and Ad Aertsen. Unitary events in multiple single-neuron spiking activity, i. detection and significance. *Neural Computation*, 14:43–80, 2001.
- [8] Sonja Grün, Markus Diesmann, and Ad Aertsen. Unitary events in multiple single-neuron spiking activity, ii. nonstationary data. *Neural Computation*, 14:81–119, 2001.
- [9] S. Nirenberg, SM Carcieri, AL Jacobs, and PE Latham. Retinal ganglion cells act largely as independent encoders. *cell*, 1:0.
- [10] Alexa Riehle, Sonja Grün, Markus Diesmann, and Ad Aertsen. Spike synchronization and rate modulation differentially involved in motor cortical function. *Science*, 278, 1997.
- [11] E. Salinas and T.J. Sejnowski. Correlated neuronal activity and the flow of neural information. *Nature Reviews Neuroscience*, 2(8):539–550, 2001.
- [12] M.N. Shadlen and J.A. Movshon. Synchrony Unbound: A Critical Evaluation of the Temporal Binding Hypothesis. *Neuron-Cambridge MA-*, 24:67–77, 1999.
- [13] William R. Softky and Christof Koch. cortical cells should fire regularly, but do not. *Neural Computation*, 4:643, 1992.
- [14] F. Varela, J.P. Lachaux, E. Rodriguez, J. Martinerie, et al. The brainweb: phase synchronization and large-scale integration. *Nature Reviews Neuroscience*, 2(4):229–239, 2001.
- [15] David K. Warland, Pamela Reinagel, Markus Meister, David K, and Pamela Reinagel. Decoding visual information from a population of retinal ganglion cells. *J. Neurophysiol*, 78:2336–2350, 1997.

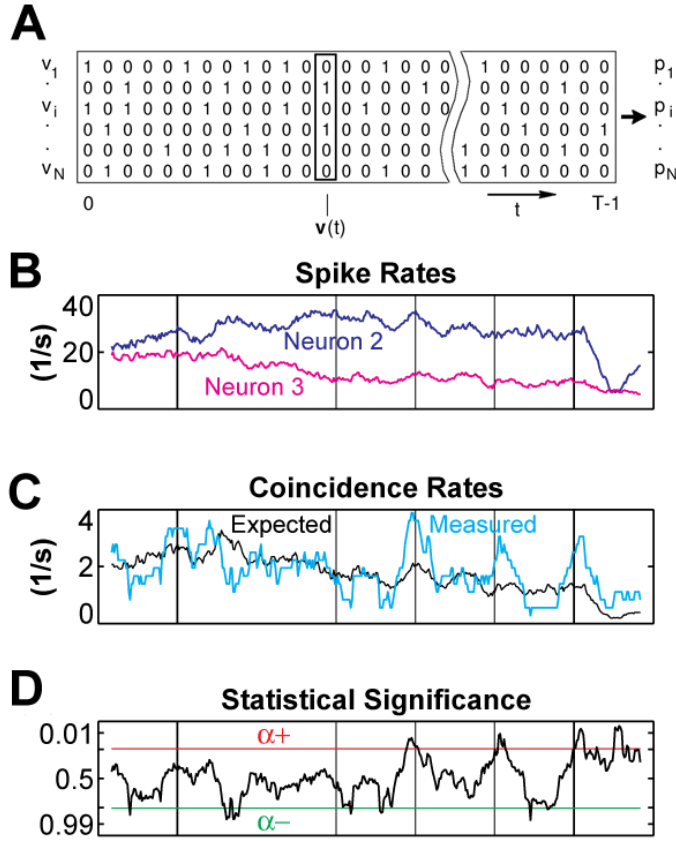


Figure 2: Unitary Event Analysis Processing Steps. (A) Spike event representation after binary binning. Each row is the binned representation of one channel. The recordings are aligned in time, each column is one $\mathbf{v}(t)$, i.e. one of the T bins. Firing probabilities p_i are calculated separately for each channel, using all spike occurrences. (B) Spike rate estimation for two recorded neurons over time. (C) Expected and measured coincidence rate over time. (D) Statistical significance with which the expected and the measured coincidence rate from (C) diverge.

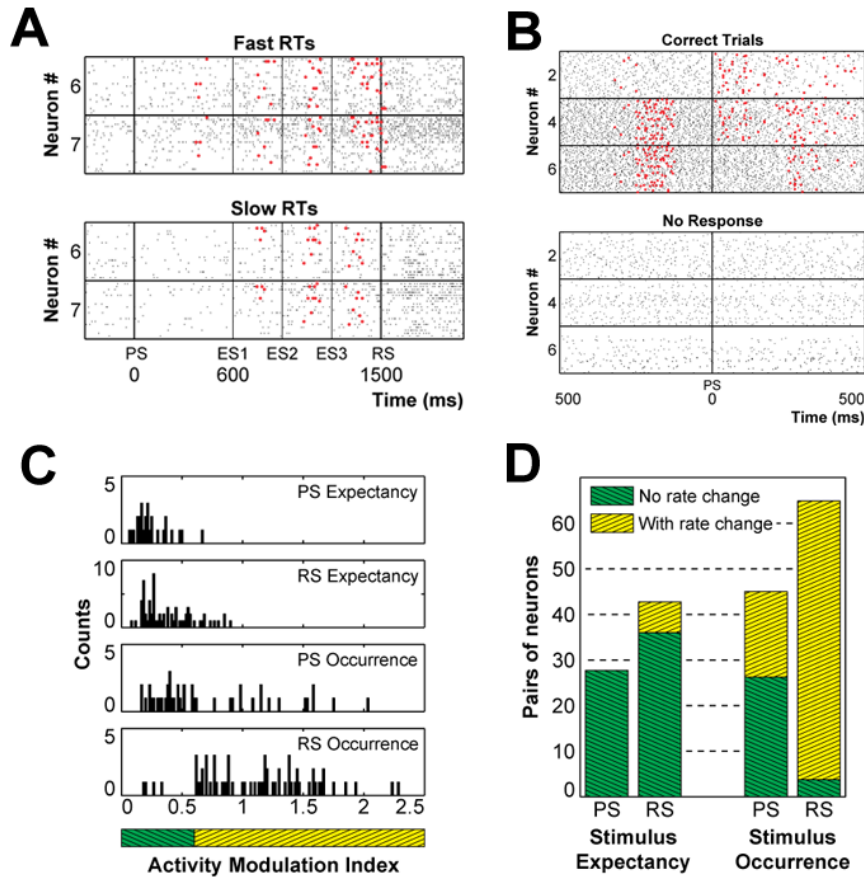


Figure 3: The main findings of Riehle et al [10]. (A, B) Relation between UEs and behavioral aspects. Occurrence of UE epochs is roughly aligned to expected stimulus time points (ES) and the coincident rate is larger for UE epochs associated with later ESs. (A) Trials with slow RTs exhibit fewer and less well clustered UE epochs. (B) Trials with correct responses from the monkeys contain clearly discernible UE epochs, whereas there are no UEs in trials in which the monkeys did not respond. Relation between stimulus occurrence and firing rate modulation in UE epochs. (C) Histogram of activity modulation index values (indicator of firing-rate modulation) in UE epochs in which a stimulus occurred (bottom two histograms) or epochs in which it was merely expected (top two histograms). The histograms were computed for the neuron in each UE pair with the strongest rate modulation. (D) Number of UEs sorted according to epochs in which the expected stimulus actually occurred and where it did not. The ratio of pairs with strong rate modulation versus without strong rate modulation is much higher in those epochs with actual stimulus occurrence.

SYNCHRONISATION OF NEURAL RESPONSES IN PRIMARY VISUAL CORTEX OF MONKEYS VIEWING NATURAL IMAGES

Pedro Maldonado, Cecilia Babul, Wolf Singer, Eugenio Rodriguez, Denise Berger and Sonja Grün first published in J Neurophysiol 100:1523-1532, 2008.

Summary Prepared by Chris Häusler (BCCN) for 'Coding with Action Potentials' – Seminar/Workshop | WS 08/09

INTRODUCTION

Many studies of the V1 visual cortex in primates have focused on neuronal responses to orientation bars and other highly controlled, somewhat unnatural stimuli. However, little is known about the processing characteristics of V1 when the subject is allowed free viewing of natural images.

In primates, on average 4 saccades are performed per second suggesting that V1 tasks such as feature extraction and scene segmentation etc. should be completed in less than 200ms. Furthermore, it has been proposed that neurons involved in early visual processing exchange only a few spikes each during analysis (GUYONNEAU ET AL. 2004). This assumption severely limits the volume of information that could be transmitted through rate coding alone and it has therefore been suggested that the early visual cortex may also employ a temporal code, encoding information in the precise timing of action potentials (FRIES ET AL. 2001, 2007; GRÜN ET AL. 2002A; HOPFIELD 2004). To date, there is no available data on the precise timing relationships between multiple spiking neurons during early visual processing.

To address this issue, this study investigates the hypothesis

“that information is encoded not only in discharge rates but also in timing relations among the spikes of individual neurons; thus we should find indications of precise timing, e.g. synchronization of discharges in these data” (MALDONADO ET AL. 2008)

METHODS

The research was performed with 2 adult male Capuchin monkey subjects. Eye coils used magnetic induction to track the precise positions of the monkeys gaze during recording sessions. A recording chamber containing 8 independently moveable tetrodes was mounted directly above V1. The tetrodes could be lowered up to 4mm into the cortex, allowing recordings at various depths and were used to perform extracellular unit recordings. All recording made while the tetrodes remained in one place were considered a recording session.

During each recording session the subjects were shown a sequence of natural images, blank images and images with a fixation cue (to ensure the subjects remained focused on the stimuli). Each eye movement event was classified as either a saccade or a fixation and considered a 'trial'. Saccades were defined as eye movements with an angular velocity greater than 100°/sec that lasted for ≥ 5 ms. Additionally, saccades were required to have an angular acceleration greater than or equal to 170°/sec². Fixations were defined as periods where the gaze remained within 1° of the position reached at the end of the last saccade for a period ≥ 100 ms. Trials were then further grouped by the viewing condition (image, blank) and the session in which they were recorded.

Based on MALDONADO ET AL. 2008.

Prepared by Chris Häusler, BCCN Berlin; for 'Coding with Action Potentials' – Seminar/Workshop | WS 08/09

A total of 80 sessions were recorded resulting in 4852 trials with images and 383 trials in the blank condition. After recording was completed, offline spike sorting was used to recreate the spike trains and 418 single units were identified. An automated offline algorithm was also used to determine and categorise the different states of eye movements (saccade, fixation) from the eye coil data.

ANALYSIS

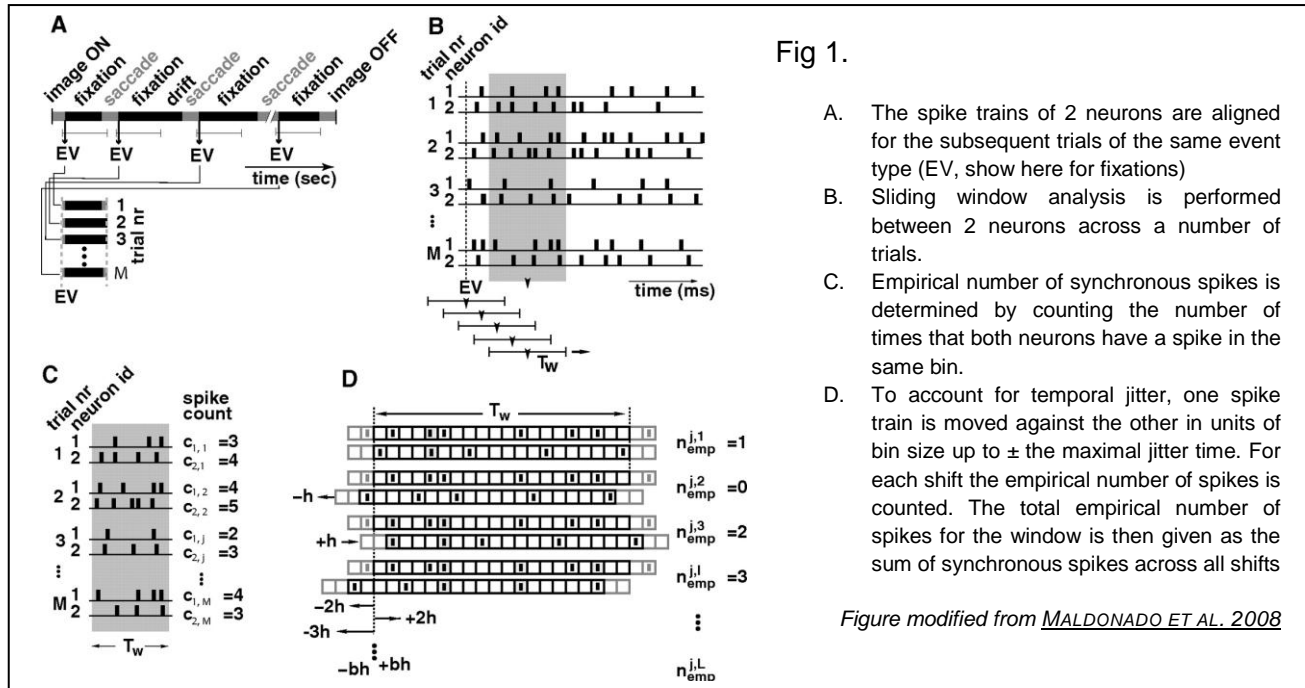


Fig 1.

- The spike trains of 2 neurons are aligned for the subsequent trials of the same event type (EV, show here for fixations)
- Sliding window analysis is performed between 2 neurons across a number of trials.
- Empirical number of synchronous spikes is determined by counting the number of times that both neurons have a spike in the same bin.
- To account for temporal jitter, one spike train is moved against the other in units of bin size up to \pm the maximal jitter time. For each shift the empirical number of spikes is counted. The total empirical number of spikes for the window is then given as the sum of synchronous spikes across all shifts

Figure modified from [MALDONADO ET AL. 2008](#)

To identify the rate of synchronous neuronal firing, Unitary Event (UE) Analysis ([GRÜN ET AL. 2002A, 2002B](#)) was applied to the recorded data. Due to non-stationary firing rates within trials, sliding window analysis ([GRÜN ET AL. 2002B](#)) with a 50ms duration and 0.1ms resolution was used. In addition, a multiple shift approach ([GRÜN ET AL 1999](#)) with up to a 5ms shift was utilised to allow for small amounts of temporal jitter in synchronous spiking. Again due to the non-stationary nature of firing rates between trials, analysis was performed on individual trials and subsequently summed and averaged across all trials to get the final results. Spike trains of neurons recorded simultaneously from the same trial were aligned and analysed in pairs against all other neurons for that particular trial. Data recorded for fixations was taken from -25ms before until 325ms after onset of the event whilst data for saccades was taken from -25ms before until 75ms after onset. Analysis of data starting at -25ms before onset was used so that the centre of the first 50ms sliding window would be aligned to time 0ms.

Based on [MALDONADO ET AL. 2008](#).

RESULTS

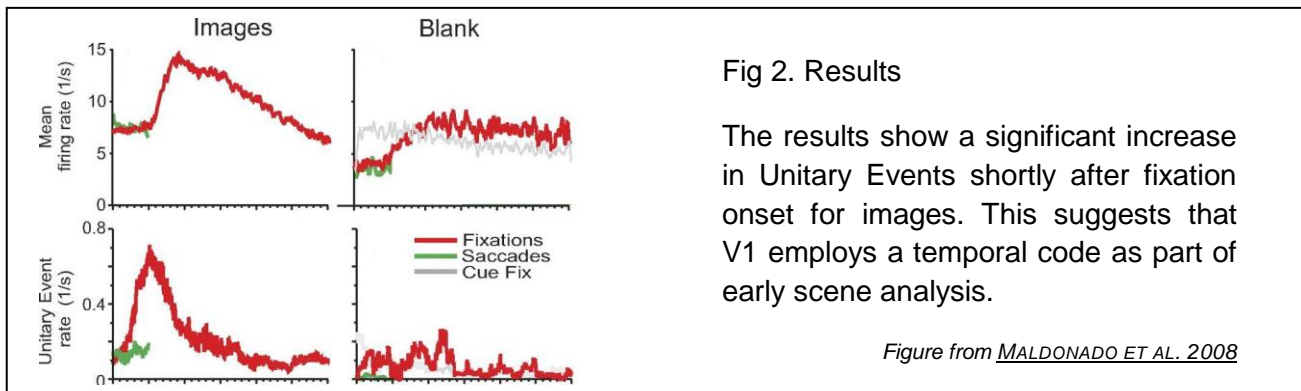


Fig 2. Results

The results show a significant increase in Unitary Events shortly after fixation onset for images. This suggests that V1 employs a temporal code as part of early scene analysis.

Figure from MALDONADO ET AL. 2008

The results (Fig 2.) clearly show a substantial increase in synchronous firing (unitary events) during image fixations, beginning at $\cong 30$ ms after onset and peaking at $\cong 50$ ms. The peak in synchronous firing occurs well before the rise in mean firing rate which does not start until $\cong 60$ ms after onset and peaks at $\cong 90$ ms. It is also important to note that there is no significant increase in the unitary event rate during saccades, cue fixations or fixations on blank images. These results strongly suggest that an active synchronisation of spike timings takes place shortly after fixation begins, supporting the theorem that a temporal code is employed in early visual processing of natural images.

CRITICISMS AND CONTROLS

It has been suggested by some critics that the increase in unitary events found during image fixation is a by-product of the rise in firing rate. The first point to make in response to this claim is that it is clear from the results (Fig 2.) that the rise and peak of the unitary event rate occurs well before any increase in mean firing rate takes place. This issue was further examined using two analytical approaches to show that the increase in unitary events is not correlated with an increased firing rate.

The first approach was to apply dithering to the recorded spike trains. The exact timing of a spike is removed by 'dithering' the spike within a dithering window whilst keeping the firing rate profile of the spike train approximately the same. That is, when dithering for ± 5 ms, all spikes in the spike train are moved to a random new time point within ± 5 ms from their original location. After dithering was applied, the data was re-analysed using the same procedure as the initial experiment. As dithering was increased from ± 0 ms to ± 50 ms, the unitary event rate shown after re-analysis rapidly decayed ($\cong 25\%$ at ± 5 ms, 50% at ± 10 ms) to a point where there was no noticeable increase in the UE rate at ± 40 ms. These results indicate that the increase in UE rate observed in the experimental results is independent of, and unrelated to, the observed increase in mean firing rate, thus suggesting that the increase in UE's is a result of an active synchronisation process.

To further substantiate this point, a second type of analysis using simulated datasets was performed. Two datasets containing spike trains for 100 neuron pairs with 100 trials per pair were generated based on the firing rate profile of the recorded experimental data. Into one of these data sets, a number of coincidences were manually injected without changing the overall firing rate of the spike train. The 2 datasets were then re-analysed using the same method as the initial experiment. The resulting analysis showed no significant

Based on MALDONADO ET AL. 2008.

change in the UE rate during fixation for the data set with no injected synchronous spikes, whilst the dataset containing injected synchrony displayed a peak UE rate almost identical to that of the original experiment. These results further support the notion that the increase in UE rate seen shortly after onset of image fixation is the result of an active synchronisation process and independent of the later increase in firing rate.

CONCLUSIONS AND FURTHER DISCUSSION

A side-effect of the spike sorting approach used in this experiment to identify single-units is that it is likely to have underestimated both the mean firing rate and UE rate. When cells being recorded by the same tetrode fire at exactly the same time, the superposition of the resulting spikes mean that the correct unit source cannot be identified and the spike must be disregarded. As a result, it is possible to have underestimated the incidence of synchronous firing by $\geq 20\%$ (MALDONADO ET AL. 2008).

In conclusion, the experimental results have shown that there is a definite and significant increase in synchronous spiking shortly after the onset of fixation when viewing a natural image. The increased synchrony is then followed by a significant increase in mean firing rate. This response pattern is unique to image fixation and is not evident during saccades, cue fixations or fixations on blank images. These results support the initial hypothesis by showing indications of an active synchronisation of spike timings. It is therefore likely that information coding during V1 scene analysis of natural images is initially handled primarily through a temporal code, with rate coding following a short time later.

REFERENCES

Fries P, Nikolic D, Singer W. The gamma cycle. *Trends Neurosci* 30: 309–316, 2007.

Fries P, Reynolds JH, Rorie AE, Desimone R. Modulation of oscillatory neuronal synchronization by selective visual attention. *Science* 291: 1560– 1563, 2001.

Grün S, Diesmann M, Aertsen A. Unitary events in multiple single-neuron spiking activity: I. Detection and significance. *Neural Comput* 14: 43–80, 2002a.

Grün S, Diesmann M, Aertsen A. Unitary events in multiple single-neuron spiking activity: II. Nonstationary data. *Neural Comput* 14: 81–119, 2002b.

Grün S, Diesmann M, Grammont F, Riehle A, Aertsen A. Detecting unitary events without discretization of time. *J Neurosci Methods* 94: 67–79, 1999.

Guyonneau R, Vanrullen R, Thorpe SJ. Temporal codes and sparse representations: a key to understanding rapid processing in the visual system. *J Physiol (Paris)* 98: 487–497, 2004.

Hopfield JJ. Encoding for computation: recognizing brief dynamical patterns by exploiting effects of weak rhythms on action-potential timing. *Proc Natl Acad Sci USA* 101: 6255–6260, 2004.

Maldonado P, Babul C, Singer W, Rodriguez E, Berger D, Grün S. Synchronisation of Neural Responses in Primary Visual Cortex of Monkeys Viewing Natural Images. *J Neurophysiol* 100:1523-1532, 2008.

Based on MALDONADO ET AL. 2008.

Prepared by Chris Häusler, BCCN Berlin; for 'Coding with Action Potentials' – Seminar/Workshop | WS 08/09

Summary

12 Thorpe, S.; Delorme, A. & Rullen, R. V. (2001) „Spike-based strategies for rapid processing.“
Neural Networks 14(6-7), 715-725

Martin Brill
Biozentrum, University of Wuerzburg
martin.brill@biozentrum.uni-wuerzburg.de

The human visual system is able to characterize images in a tremendously short time period ranging from 100-150ms. To elucidate how this short period is sufficient to process 3D images in higher cortical visual neurons Thorpe and colleagues (Thorpe *et al.*, 2001) compared different coding strategies that could underlie this mechanism and that can be implemented in computer algorithm for visual processing like face tracking.

At first to reveal these short time periods Thorpe and colleagues (Thorpe *et al.*, 1996) analyzed test persons that had to distinguish images showing animals from images with natural scenes. In this so called go/no-go characterization task they showed that a precise (94% in average) decision-making of the probands on 'go' trials (i.e. animal) was achieved after 445ms, meaning the test person pressed the right button 445ms after stimulus onset. But to crystallize the visual decoding process from decision making and motor control they recorded evoked potentials extracellularly from the head of the test persons (EEG). Already 100-150ms after the stimulus emerged on a small computer screen event-related potentials could be measured. Also in other go/no-go characterization tasks such as distinguishing faces from natural scenes higher cortical neurons in the human visual system were recorded and showed event-related potentials again 100-150ms after stimulus onset (Antal et al., 2000; Thorpe et al., 1983). This so called Ultra-Rapid Visual Characterization (URVC) has certain distinct features: 1. URVC works colorblind, i.e. monochromatic images are processed very efficiently (Delorme *et al.*, 2000), 2. there is no difference in the characterization task whether the images are familiar or totally novel, indicating that contextual information is largely unnecessary (Fabre-Thorpe *et al.*, 2001), 3. it is unaffected by biologically relevant images (VanRullen and Thorpe, 2001) and finally, it does not require direct fixation on the object, since it works well in parafovea vision (Fabre-Thorpe *et al.*, 1998).

After Thorpe and colleagues (1996) defined the URVC in humans they were interested how the visual system is able to convey neuronal excitation in less than 150ms from the photoreceptors of the retina to the higher cortical areas that are LGN, V1, V2, V4 and finally to the infero-temporal cortex that is responsible for identifying objects (Mishkin *et al.*, 1983); especially considering that this certain anatomical pathway needs at least 10 synaptic stages (Thorpe & Imbert 1989) (Thorpe and Imbert, 1989). Taking the overall time of 100-150ms and the ten stages in mind it results in remaining 10ms to encode stimulus information (Gautrais and Thorpe, 1998).

First of all Poisson-like rate codes that are typically used to analyze neuronal processes were considered as approximations to neuronal decoding and whether it might be sufficient in URVC tasks processing (Gautrais and Thorpe, 1998), although a Poisson process is just a simplification and even

ignores known intrinsic neuronal properties e.g. refraction time (Thorpe *et al.*, 2001). The firing rate that underlies the assumed time period of ten ms that remains for each neuronal level, with a confidence interval of 90%, lies at 5-472 Hz (Gautrais and Thorpe, 1998). To increase this obviously insufficient knowledge about the firing rate there remain two possibilities namely increasing the processing time of each neuron, which apparently does not work, or to increase the amount of neurons per level. Following on from this, to obtain a precision of up to 100 ± 10 Hz firing rate one would require 281 neurons. Taking into account the optical nerve only resembles 1 Mio neurons and is subdivided in neurons that code e.g. for on- or off- responses, the retina would convey the information of an image to higher brain regions with just 30 x 30 points resolution. Obviously rate coding does not seem to be convenient to be the underlying mechanism for rapid visual processing. Therefore alternative coding schemas were considered likely to be responsible for URVC.

One option would be to just **count the number of neurons** that have spiked during a particular time window. According to the example shown in Fig. 1 nine out of ten neurons fired during a ten ms interval or 90 spikes per s. With such a coding scheme the maximum amount of information that can be transmitted during 10ms would be equal to $\log_2(N + 1)$ bits, where N is the number of neurons, since there are only $N + 1$ possible states of the system. The upper limit of the system by using ten neurons would be 3.46 bits (Thorpe *et al.*, 2001).

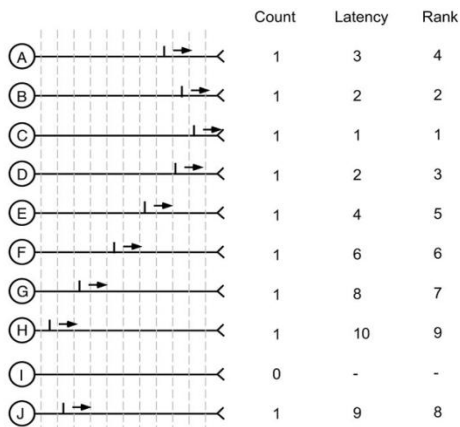


Fig. 1: Comparison between three coding schemes that can operate in a short time period, here 10ms. The 10 Neurons A-J spike with different times. By using a count code, corresponding to a population rate code, there are only 10+1 states of the system. If the latency of each spike can be determined with ms precision, there are 10^{10} possible states. Finally, with rank code, there are 10! possible states. (adapted from Thorpe *et al.* 2001)

Another more efficient possibility to encode ten neurons during a 10ms time window would be a **bit-like counting** of neuronal responses. Each neuron that has spiked would get a count 1, each that does not get a 0. By using the example introduced in Fig. 1 i.e. 1111111101, that would be one of 1024 possibilities. The maximum amount of information with N neurons would be $\log_2(2^N) = N$ bits. The increase in information compared to the rate is compensated by considering that the binary code is strongly time dependent.

The most precise decoding algorithm would be to determine the precise **timing** of the spike, or latency respectively. Therefore the decoding scheme is restricted to the resolution in time, the higher the temporal resolution gets the higher the amount of information becomes. Regarding the example and applying a temporal resolution of 1ms one would get a maximum amount of information in t ms of $N * \log_2(t)$ bits = 33 bits. This powerful encoding mechanism has the disadvantage of high energy consumption to implement such a precise neuronal architecture.

A less powerful but compared to the timing code less energy consuming coding mechanism would be to analyze the **order** of incoming spikes. Regarding the example in Fig. 1 the first spike that comes from

neuron 'C' would get the order of 1 the second neuron, neuron 'B', would get the order of 2 and so on. The output order of the example then would be C>B>D>A>E>F>G>J>H>I. Rank order coding would implement a maximum amount of information of 10! that would be 3.6Mio possibilities with 10 neurons. The transmitting rate would be $\text{Log}_2(N!)$ bits of information, regarding the experiment which would be 20 bits.

A final conceivable coding scheme resembles the **synchrony coding**. Therefore groups of neurons that are timely linked together are handled in groups. In respect to the grouping size, the amount of information increases. If there were three different timely linked spiking groups they could transmit 4^{10} patterns. The maximal amount of information would be $\text{Log}_2(4^{10})$ bits that equals 20 bit.

In Summary the best coding mechanism seems to be the rank order coding because compared to the other schemes it is less complex but still in a high range of information transmission.

But not only the transmission and decoding of information from the retina to higher cortical processing stages should be taken into account if analyzing rapid visual processing. Also the input site of the retina should be discussed. The authors (Thorpe *et al.*, 2001) argue stimulus processing is most suitable if considering the correlation of stimulus intensity and latency. That means strong stimuli will generate high EPSPs in the retinal ganglion cells and consequently generate spikes earlier whereas low intensity stimuli will generate weaker EPSPs and spike generation will be delayed, respectively.

Regarding the integrate and fire properties of retinal ganglion cells, in response to a flashed stimulus, the neuron will tend to fire in an order that reflects the spatial characteristics of the image. Thus, the order of firing in the optic nerve could be used to encode the image. The rank order coding scheme therefore resembles a highly sufficient way to decode the stimulus intensity. This can even be implemented in computer software like SpikeNet (VanRullen *et al.*, 1998), giving each neuron a weighting regarding its order, i.e. those cells that fire first are given a high weighting, whereas those that fire later are given less and less importance. For instance already after 1-2% of all cells have fired an almost finely structured image can be resolved (Thorpe *et al.*, 2001; VanRullen *et al.*, 1998).

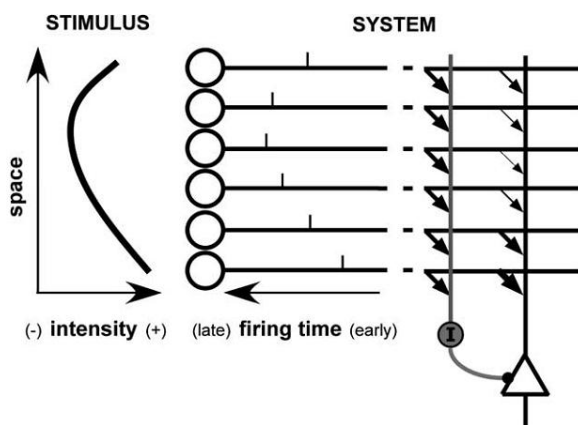


Fig. 2: A simple circuit showing shunting inhibition for rank order coding. A pyramidal neuron (triangle cell) receives excitatory input from the afferents unit through synapses with variable weights regarding their intensity they code for. Neuron "I" gets excitatory input from the same units but with equal weight. This inhibitory cell generates shunting inhibition that progressively desensitises the pyramidal cell as more and more the input fires. First inputs are effective while later ones are attenuated. (Guyonneau *et al.*, 2004)

A more biologically relevant example for implementing the rank order algorithm resembles a feed-forward network with shunting inhibition seen in Fig. 2 (Gautrais and Thorpe, 1998; Guyonneau *et al.*, 2004). In this model the output neuron that resembles the next processing stage in the visual cortex gets rank order input of neurons weighted regarding their stimulus input. Also the input neurons excite a local interneuron with equal weight. This inhibitory neuron provides shunting inhibition. As a result

leading spikes will be transmitted to the next neuronal stage without attenuation whereas the other are attenuated regarding their rank order. This model has been even been tested in the visual system (Callaway, 1998; Delorme, 2003). Regarding the rank order coding together with this model it is a powerful schematic to decode rapid visual stimuli and it even is able to implement learning models (Guyonneau *et al.*, 2004) for example, introducing synaptic plasticity or certain thresholds in the target cells at the next processing stages. Therefore based on this rank order shunting inhibition model face recognition algorithm applied in software is working sufficiently well (Delorme and Thorpe, 2001).

These analyzed underlying mechanism of rank order coding and shunting inhibition seem to be a powerful model for rapid visual processing.

- Antal, A., Keri, S., Kovacs, G., Janka, Z., Benedek, G., 2000. Early and late components of visual categorization: an event-related potential study. *Brain Res Cogn Brain Res.* 9, 117-9.
- Callaway, E. M., 1998. Local circuits in primary visual cortex of the macaque monkey. *Annu Rev Neurosci.* 21, 47-74.
- Delorme, A., 2003. Early cortical orientation selectivity: how fast inhibition decodes the order of spike latencies. *J Comput Neurosci.* 15, 357-65.
- Delorme, A., Richard, G., Fabre-Thorpe, M., 2000. Ultra-rapid categorisation of natural scenes does not rely on colour cues: a study in monkeys and humans. *Vision Research.* 40, 2187-2200.
- Delorme, A., Thorpe, S. J., 2001. Face identification using one spike per neuron: resistance to image degradations. *Neural Networks.* 14, 795-803.
- Fabre-Thorpe, M., Delorme, A., Marlot, C., Thorpe, S., 2001. A limit to the speed of processing in ultra-rapid visual categorization of novel natural scenes. *Journal of Cognitive Neuroscience.* 13, 171-180.
- Fabre-Thorpe, M., Richard, G., Thorpe, S. J., 1998. Rapid categorization of natural images by rhesus monkeys. *Neuroreport.* 9, 303-308.
- Gautrais, J., Thorpe, S., 1998. Rate coding versus temporal order coding: a theoretical approach. *Biosystems* 48, 57-65.
- Guyonneau, R., VanRullen, R., Thorpe, S. J., 2004. Temporal codes and sparse representations: A key to understanding rapid processing in the visual system. *Journal of Physiology-Paris.* 98, 487-497.
- Mishkin, M., Ungerleider, L. G., Macko, K., Object Vision and Spatial Vision: Two Cortical Pathways. In: W. Bechtel, P. Mandik, J. Mundale, R. Stufflebeam, (Eds.), *Philosophy and the Neurosciences.* Blackwell Publishing, 1983.
- Thorpe, S., Delorme, A., Van Rullen, R., 2001. Spike-based strategies for rapid processing. *Neural Networks.* 14, 715-725.
- Thorpe, S., Fize, D., Marlot, C., 1996. Speed of processing in the human visual system. *Nature.* 381, 520-522.
- Thorpe, S., Imbert, M., Biological constraints on connectionist modelling. In: R. Pfeifer, Z. Schreter, F. Fogelman-Soulié, L. Steels, (Eds.), *Connectionism in perspective.* Elsevier, Amsterdam, 1989, pp. 63-93.
- Thorpe, S. J., Rolls, E. T., Maddison, S., 1983. The Orbitofrontal Cortex - Neuronal-Activity in the Behaving Monkey. *Experimental Brain Research.* 49, 93-115.
- VanRullen, R., Gautrais, J., Delorme, A., Thorpe, S., 1998. Face processing using one spike per neurone. *Biosystems.* 48, 229-39.
- VanRullen, R., Thorpe, S. J., 2001. The time course of visual processing: From early perception to decision-making. *Journal of Cognitive Neuroscience.* 13, 454-461.

Rapid Encoding and Perception of Novel odour in the Rat

Authors: DW Wesson, RM Carey, JV Verhagen and M Wachowiak
Journal: PLOS Biology, Volume 6, Issue 4, April 2008

Summary written by Johannes Felsenberg, Freie Universität Berlin

The capacity of the brain to process information is limited by the number of neurons in the corresponding neuropil. If a neuron is able to carry more than one signal simultaneously, it would increase the total information processing potential of the neuropil. So far, the data indicates that this could be realized by two parameters: first the spike count and second the precise times of spikes relative to stimulus onset (response latency) (Oram et al. 2002). The present research of Wesson et al. is addressing the question what parameters of activity are important for shaping the perception of unlearned odours in rats. To do so they combined a behavioural measure of odour perception with the optical imaging of olfactory receptor neurons (ORN) input onto the olfactory bulb (OB) of rats (Figure 1).

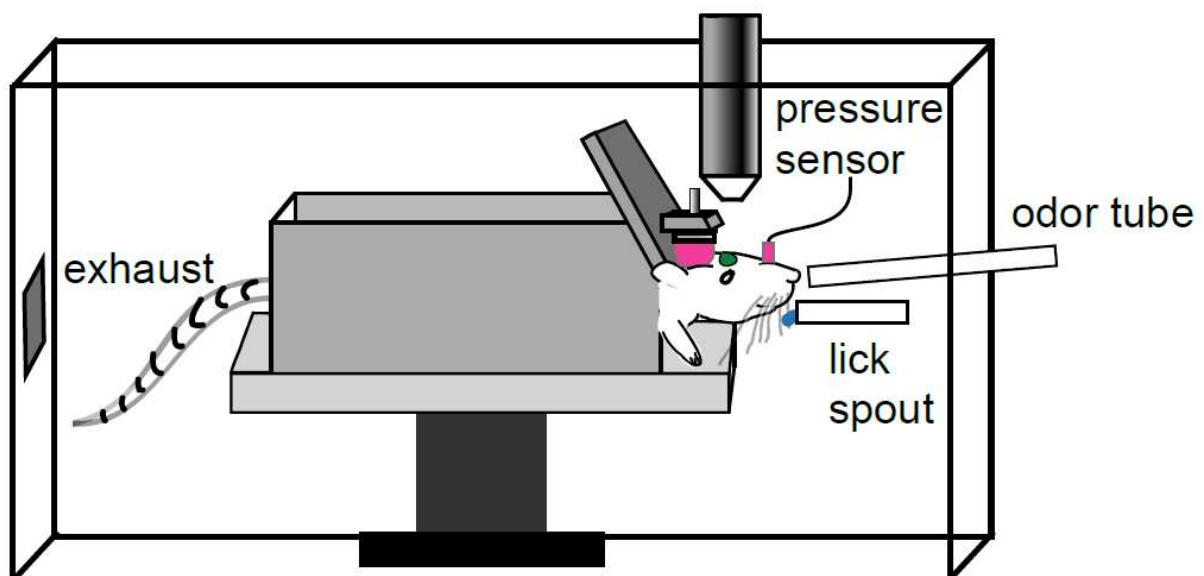


Figure 1: Schematic of the head-fixed behavioural apparatus. Shown is a rat in an acrylic chamber with its head bolt (pink) clamped to a steel tab. In front of the animal are a lick spout and odour tube, and above the olfactory bulb window (green) is the objective. Sniffing is measured via an intranasal cannula (pink) communicating with a pressure sensor. This setup is enclosed in a black box with a fan for odorant removal (Verhagen 2007, Supplementary Fig.1).

They analysed the timing of an ethologically natural odour discrimination behaviour: the exploratory sniffing to a novel odorant. This allows the authors to measure the time course with which rats can perform odour discrimination. They confirm previous findings that rats can identify an odour as novel rapidly ($< 200\text{ms}$) after the first inhalation (Behavioural response in Figure 2). Concurrently to the behavioural performance Wesson and his colleagues were measuring the ORN input to the dorsal OB via Ca^{2+} -imaging. These data show that the receptor input arrives at the OB 100 -150ms after the first inhalation (t_{onset} in Figure 2). They likewise show that the maximal signal amplitude of the whole neuropil is reached after the behavioural response occurs (t_{90} in Figure 2).

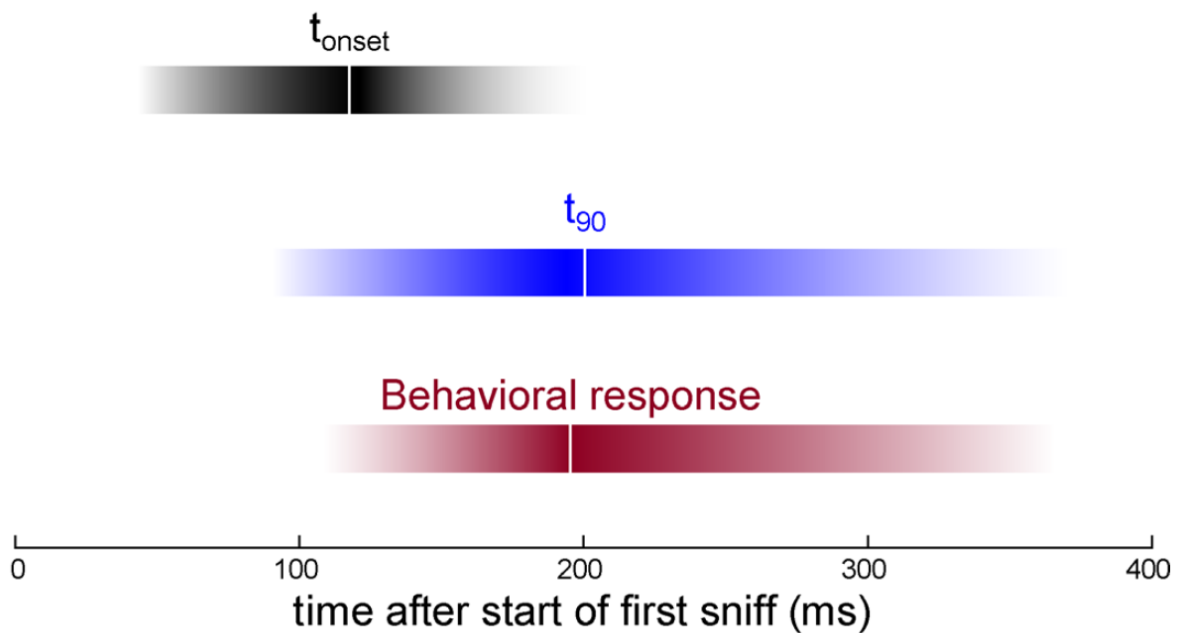


Figure 2: Schematic summarizing the dynamics of neural activity and behavioural responses after the first inhalation of a novel odorant: t_{onset} , time to the earliest arrival of receptor input at the olfactory bulb; t_{90} , time to 90% signal amplitude for the optical signal in all glomeruli; behavioural response, time to the next inhalation for novel-odorant trials. Solid bars are representations of the probability of occurrence for each parameter. Darker colour indicates increased probability. The median is indicated by the white line in the centre of each bar (present Publication, Wesson et al. 2008).

These time course leaves as few as 50-100ms for central processing and response initiation. On the basis of these results the authors discuss different existing models of odour identity encoding. They argue that their results suggest, that the encoding by activity maps focused on the peak or time-integrated activity, may be unreliable representatives of the patterns of neural activity occurring at the time of odour discrimination. Beyond they state that the little span left for central processing sharply limits the role that coding strategies based on changes in firing rate can play in odour discrimination. In contrast Wesson's results support models in which the relative timing of activation of glomeruli (e.g. sequence) or only the earliest-activated glomeruli encodes the odour identity.

Literature:

Oram MW, Xiao D, Ditschel B, Payne KR (2002) The temporal resolution of neural codes: does response latency have a unique role? *Philos Trans R Soc Lond B Biol Sci.* 2002 Aug 29;357(1424):987-1001. Review.

Verhagen JV, Wesson DW, Netoff TI, White JA, Wachowiak M (2007) Sniffing controls an adaptive filter of sensory input to the olfactory bulb. *Nat Neurosci.* 2007 May;10(5):631-9. Epub 2007 Apr 22.

Wesson DW, Carey RM, Verhagen JV, Wachowiak M (2008) Rapid encoding and perception of novel odors in the rat. *PLoS Biol.* 2008 Apr 8;6(4):e82.

Representation of multiple stimulus dimensions in rate and temporal codes of single neurons

Vinzenz Schönfelder – BCCN Berlin & TU Berlin

February 6, 2009

1 Introduction

The text at hand presents a paper by medicine grad student Steven M. Chase and professor Eric D. Young, originally a biomedical engineer, both at Johns Hopkins University, Baltimore, entitled "*Spike-Timing Codes Enhance the Representation of Multiple Simultaneous Sound-Localization Cues in the Inferior Colliculus*" [2].

They consider the question how multiple stimulus features are represented in individual neurons using the example of auditory localisation by loudness cues (ILD), temporal cues (ITD), spectral cues (SN="spectral notch"). They analyse a brain structure in the auditory pathway, where these three cues converge: the central nucleus of the inferior colliculus (ICC). The study considers the coding of these cues by both spike rate and spike timing in individual neurons as well as interactions/independence of these representations.

2 Concepts and Theoretical Methods

Chase and Young use a recent spike distance metric (SDM) [5] to estimate the mutual information between the temporal structure of spike trains and particular sound features.

Spike Distance Metric

The similarity of or distance between spike trains in the SDM framework is measured as the number of three elementary steps to generate one spike train from another: addition and elimination, as well as temporal shifting of individual spikes.

A single trade-off parameter q determines the relative cost of shifting vs. elimination&addition of a spike: spikes at a distance below $2/q$ are shifted into alignment, while higher delays result in spike removal and introduction of a new spike.

At $q = 0$, when shifting spikes has no costs, SDM equals a rate code since costs only arise from a different total number of spikes. At the other extreme end, at high q 's, shifting spikes is very costly – the distance metric acts as a coincidence detector, for spikes that don't exactly coincide, are not associated.

Note that the absolute temporal alignment of spike trains is critical with this measure: the exact same spike train, shifted only for a fraction of a microsecond may result in higher costs than missing or additional spikes. If spike train alignment within fractions of milliseconds is not guaranteed, this may be considered a weak point of the distance metric. In this study, spike trains are aligned according to stimulus onset.

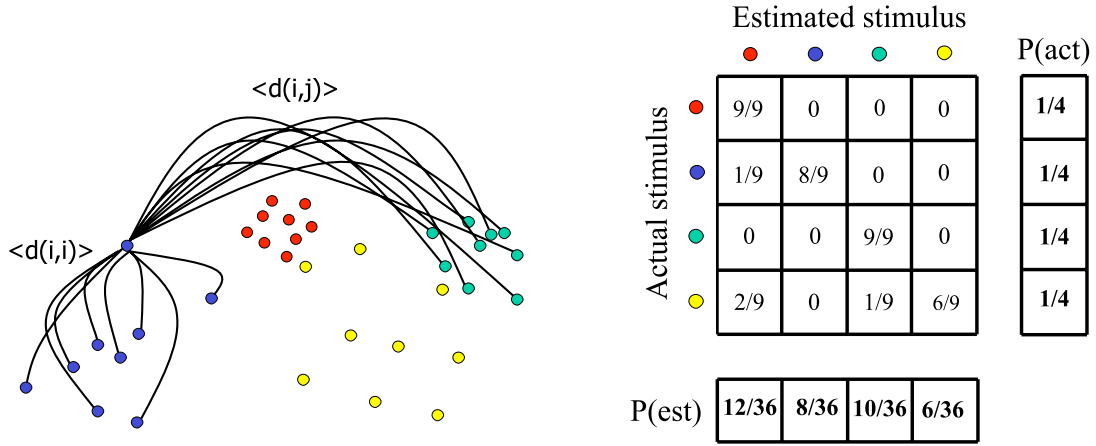


Figure 1: Characterisation of spike trains according to the SDM distance: **Left** Each dot represents a spike train, the lines spike train distances, colour depicts different stimuli. **Right** The corresponding confusion matrix describes stimulus specificity of the spike trains, $P(act)$ and $P(est)$ represent the marginal probabilities.

Mutual Information

As the name implies, mutual information (MI) measures the mutual dependence of two random variables, "how much knowing one of these variables reduces our uncertainty about the other" [wikipedia].

The definition of MI [3]

$$MI(x; y) = \sum_x \sum_y p(x, y) \log \frac{p(x, y)}{p(x)p(y)}$$

results in a measure ranging from 0 for *independent* variables [$p(x, y) = p(x)p(y) \rightarrow MI(x; y) = 0$, "one variable doesn't provide any information about the other"] to the entropy H (the measure of uncertainty of one variable) in case of "*super-dependent*" variables [$x=y \rightarrow p(x,y)=p(x)=p(y) \rightarrow MI(x; y) = -\sum_x p(x) \log p(x) = H(x)$, "one variable tells everything there is to know about the other"].

Chase and Young first calculate MI between spike trains and stimuli assuming a rate code: $p(x,y)$ is then simply the probability of getting a rate count x given stimulus y , $p(x)$ the probability of getting rate count x disregarding the stimulus, and $p(y)$ the probability (or relative frequency) of stimulus presentation y .

Confusion Matrix

Using SDM, the specificity of spike trains to particular stimuli is calculated. Therefore, spike trains are recorded during the presentation of different stimuli. Thus, each spike train has an *actual stimulus*, it was elicited by.

Inversely, given the spike train, one can *estimate* what the corresponding stimulus was: For each spike train i the average distance to all spike trains elicited by the stimulus j is calculated ($\langle d(i, j) \rangle$ according to SDM). The spike train is then estimated to result from that stimulus that generated on average the nearest spike trains, as sketched in figure 1 (left).

Hence, as similar stimuli commonly result in similar spike trains, most spike trains will finally have the same *actual* and *estimated* stimulus, but a few will be assigned to a different stimulus. Actual and estimated stimulus will be "confused", e.g. the two upper left yellow spike trains in figure 1 will be assigned to the red stimulus. The results are expressed in a confusion matrix as depicted in figure 1 (right). The larger the values on the matrix diagonal, the more specifically are spike trains associated with their eliciting stimulus.

Integrating Confusion Matrix and Mutual Information

Young and Chase finally employed the matrix to calculate MI between stimuli and spike trains assuming a temporal spike code: With s the *actual* and r the *estimated* stimulus, $MI(s, r)$ is calculated using the entries

$p(s, r)$ and marginals $p(r)$, $p(s)$ of the confusion matrix. Notice that the SDM and thus the confusion matrix as well as MI are all a function of the SDM cost variable q !

There are three assumptions in this method: 1) Information is carried by the absolute timing of spikes with whatever temporal reference one chooses. 2) Every spike carries (more or less) the same amount of information, since all receive equal weight in SDM. 3) Information is carried in the spiking pattern of single neurons. These assumptions may or may not hold for information processing in the brain.

3 Experiments and Results

During the electrophysiological experiment, artificially generated sounds, that vary in two of the above mentioned localisation cues, are presented to decerebrated adult cat. Single neurons are recorded in ICC, the stimulus length ranges between 200-400 ms. First, the stimuli are generated as *frozen noise*, i.e. the exact same noise sample (with different localisation cues) is repeatedly presented in all trials.

The paper presents the results for different combinations of the localisation stimulus features: ITD, ILD and SN. Assuming either a rate code or a temporal code, the MI between individual and combined cues and the spike trains are then estimated. Second, the study addresses the question whether different stimulus features are independently represented. Here, the results will be discussed for one example depicted in figure 2 with stimuli varying in both ILD and ITD cues.

Rate code MI

The surface plot in A shows the spike rate dependence from both cues. The surface is relatively flat, thus spike rate alone does not provide much information about the stimulus, only 0.3 bits. However, using the SDM metric, up to 1.6 bits of mutual information with both localisation cues (plot C) can be extracted, depending on the cost parameter q . Note that, for $q = 0$, the SDM degenerates to a rate code-distance and, indeed, MI reaches the same value (0.3 bits) as for the rate code analysis above.

Temporal Code MI

The mutual information of spike train and the individual stimulus cues (plots D, E) is generally smaller than for both features combined (which is a theoretical fact, as Chase and Young prove in an earlier paper [1]). Specifically, there is very little mutual information between the ITD cue and the spikes. This corresponds well with the observations in the raw spike trains presented in figure 2B: a consistent activation of the first and a continuous shift of the following spike burst for increasing ILD values, while there are no such obvious differences, for different ITDs. Even with SDM, not much spike train information about ITD can be extracted.

The study also presents neurons, where spike timing does not add much to the information provided by spike rate. In general, neurons show a behaviour between these extremes, while specific neuron types receive higher gains than others. In all cases, ITD cues are poorly reconstructed from temporal spike information just as in the example in figure 2E. Consequently, the authors suggest that ITD is carried in a rate code at the level of the ICC. On the other hand, ILD and particularly spectral cues are significantly better represented in temporal than in rate codes in many neurons.

Temporal precision of spike trains

Considering the value of q that produces the peak MI and given that q determines the delay between spikes when they are aligned or replaced, the authors estimate the temporal precision of the spike code: For all measured neurons the median value (ignoring $q = 0$ values) is about 80/s, which corresponds to roughly 12 ms in temporal resolution. This only shows that the combination of MI and SDM is best at extracting information at this temporal scale. That is not a proof, though, that the neural system operates at this time resolution.

Frozen vs. Random noise

These results should also not mislead the reader into thinking that information about the specific localisation cues in the stimuli is actively encoded in complicated firing patterns. Remember that, so far, all data resulted from frozen noise stimuli, thus not only the localisation cues are constant for different presentation epochs, but the entire sound pattern of the stimulus.

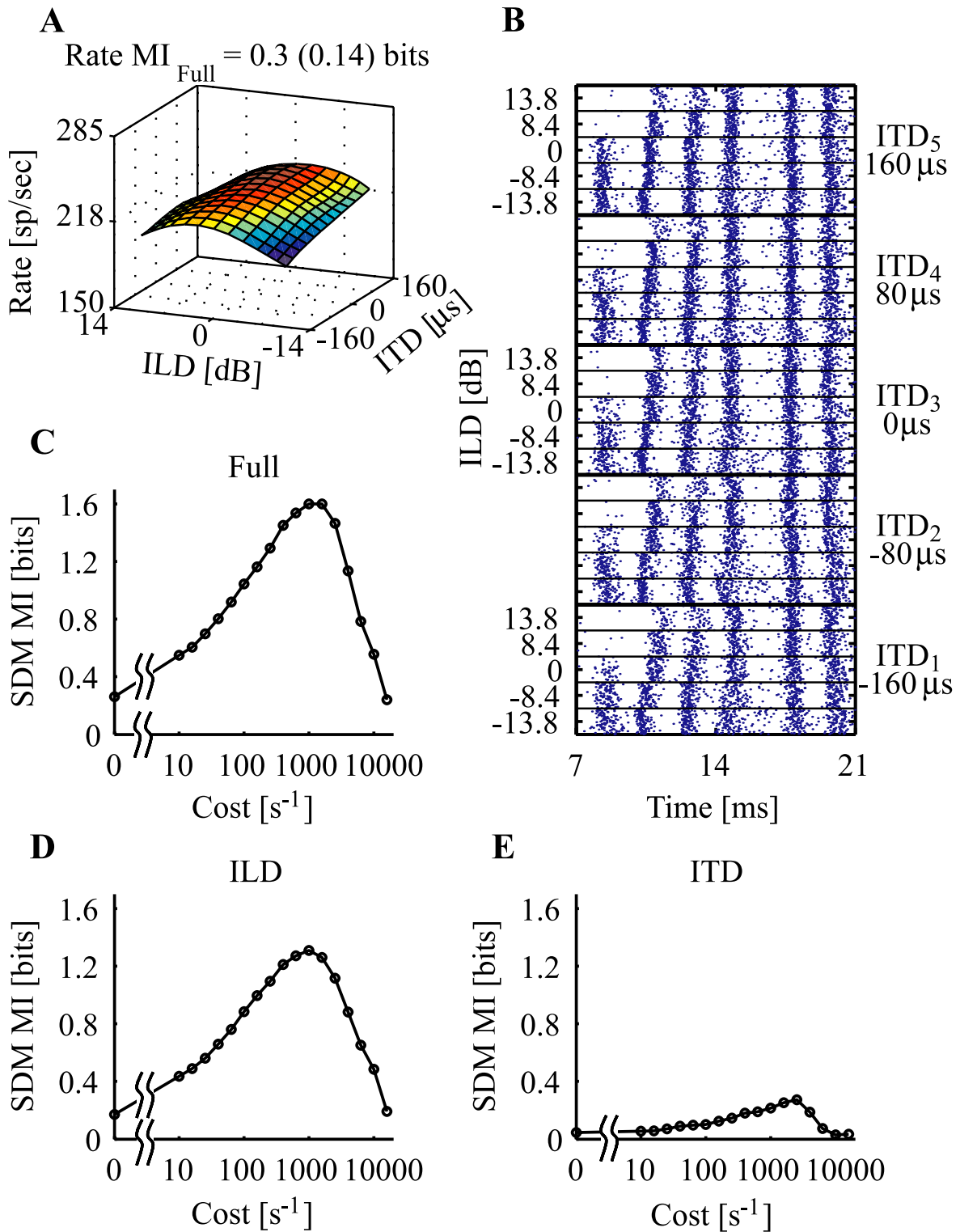


Figure 2: **A** spike rate as a function of ILD and ITD localisation cue and extracted mutual information between spike rate and both cues, **B** raw spike trains aligned to stimulus onset for different ITD/ILD combinations, **C** MI between both stimulus cues and SDM (temporal spike code) as a function of the cost parameter q , **D**&**E** MI between SDM and the individual localisation features as function of q

To address this issue, the authors introduce a different condition: the noise stimuli were varied by randomizing fourier phases (*but not amplitudes*), thus randomising temporal (*but not spectral*) structure, the localisation cues are not altered by this manipulation. While the randomisation results in very little difference in the average rate response, the stable temporal structure of the spike trains across different presentations (as observed in figure 2B) is completely broken, apart from first spike latencies.

It is obvious, that the neurons responded to specific temporal events in the stimuli in the frozen noise condition. Thus, the gain of information about the localisation features by considering spike timing is mainly attributable to the differences in temporal waveforms. After removal of temporal waveform information, the SDM method fails to extract localisation features from the spikes.

Independent representation of stimulus information

Finally, by introducing the notion of confounded information, the authors consider the interaction of different cues in the spike trains. Confounded information is defined as the difference between the MI for all cues combined and the MI for each individual cue $MI_{conf} = MI_{full} - MI_{cue1} - MI_{cue2}$. It was shown [4; 1], that if $MI_{conf} = 0$, all stimulus cues can be decoded independently from the spike train.

As expected, with a uni-dimensional rate code, multi-dimensional cues do show a confounded representation in the spike train. Adding spike timing information, multiple cues can however be represented (and decoded) more independently. The authors find that for $q = 50/s$ and above, MI_{conf} vanishes, thus SN and ILD cues are coded independently, at larger q 's information about both cues decreases gradually.

4 Conclusions

The present study demonstrates, how temporal codes are able to transmit independent and more informative stimulus data as compared to rate codes. The random noise results suggest, that differences in the temporal spike train representation of stimulus features is mainly attributable to temporal changes in the stimuli, not to active encoding of stimulus information by neural processing. It remains unclear, whether neurons indeed use timing information independent of the temporal structure of the stimuli, to transmit stimulus features.

The authors acknowledge, that the SDM method is largely insensitive to first spike latencies, although they may contain more critical information. The reason is, that all spikes are weighted equally. The case, where some spikes may be more informative than others, is ignored in the present metric.

Finally, the employed methods are limited to absolute spike timing/coincidence and rate code, but e.g. not to the relative position of spikes, or spiking patterns of multiple neurons. The authors consider their results mainly as a lower bound on information available in single spike trains. Whether the neural system relies on the same (temporal and rate) cues, that were considered in this study, remains open.

References

- [1] Steven M Chase and Eric D Young. Limited segregation of different types of sound localization information among classes of units in the inferior colliculus. *The Journal of neuroscience*, 25(33):7575–85, Aug 2005.
- [2] Steven M Chase and Eric D Young. Spike-timing codes enhance the representation of multiple simultaneous sound-localization cues in the inferior colliculus. *The Journal of neuroscience*, 26(15):3889–98, Apr 2006.
- [3] Thomas M Cover and Joy A Thomas. *Elements of information theory*. Wiley, New York, 1991.
- [4] D S Reich, F Mechler, and J D Victor. Formal and attribute-specific information in primary visual cortex. *J Neurophysiol*, 85(1):305–18, Jan 2001.
- [5] Jonathan D Victor and Keith P Purpura. Metric-space analysis of spike trains: theory, algorithms, and application. *Comput. Neural Syst.*, 8:127–164, Oct 1997.

IMPORTANT NOTES

Please **select 3 specific topics** (out of 14) that you are interested. No.1 should be most interesting and No.3 is least interesting. We will then assign the individual participants of the specific topics. Send selection via Email to M Nawrot AND M Schmuker.

Note: All **Master/Diplom students** will be assigned to a tutor who helps the student to understand the literature, prepare the talk and the summary. **Meeting with her/his tutor is mandatory** in January 2009.

Note: **PhD Students** are expected to prepare both, summary and presentation on their own. However, they may request help if they do not fully understand the literature or the methods used therein or they may discuss the problems with other participants of their institute.

Oral presentation (~20 minutes + max. 10 min for additional methods) need to consider methods, results, conclusions. We will encounter several central experimental methods and principle models. These are marked in **blue** where they show up first. This means that the respective presenter(s) must provide an introduction to that method. Understanding fundamental methods is also one important teaching goal of this seminar. There will be additional time for discussion of the topic after each presentation (approx. 10 min). Note, our experience is that most speakers usually needs *more* time than planned. Try to restrict yourself on 20 minutes + max. 10 minutes for **blue** methods and be prepared for questions in the discussion.

Written summary should be of 2-4 pages (11pt Arial) in length with max. 2 figures. It should mention the methods used and briefly relate the relevant experiments, summarize the results and conclusions, give a short reference to the original papers and further literature that was used for the summary/presentation. Please hand in final version **latest by Feb 8** as PDF. Please discuss a draft version with your tutor before that date.